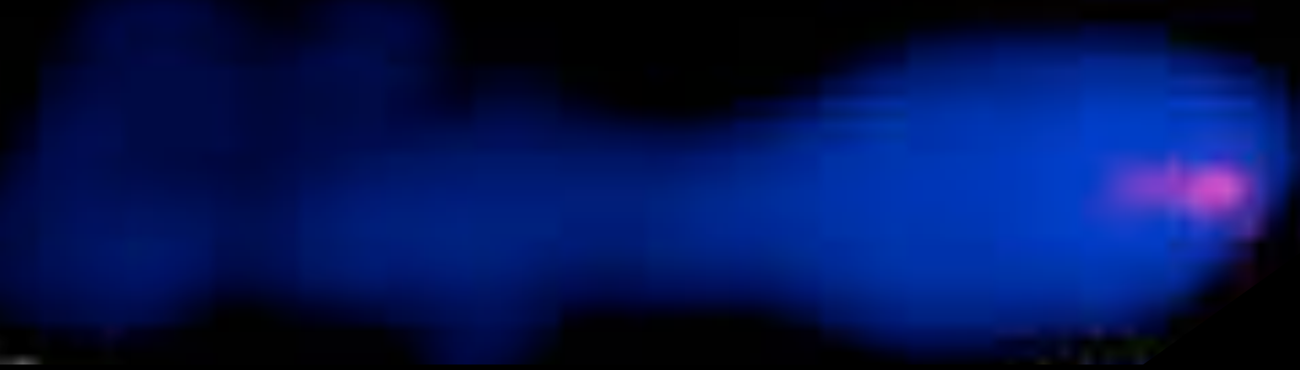

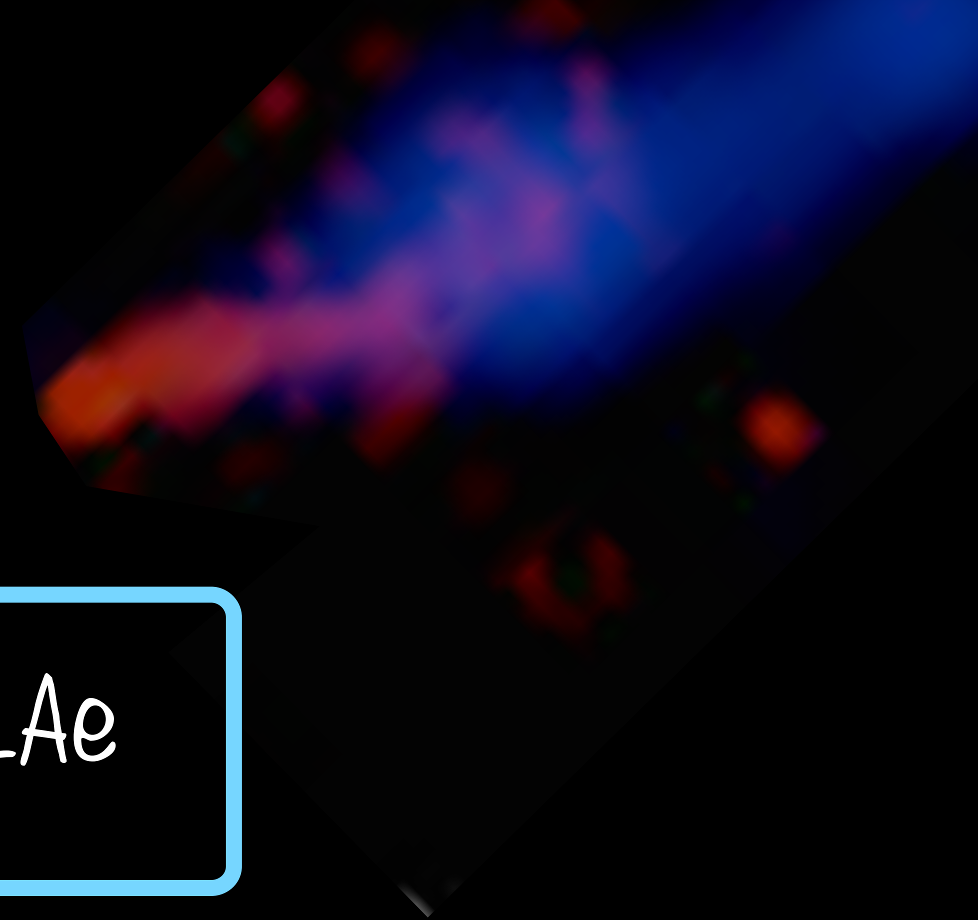

EVOLUTION of PULSAR WIND NEBULAe

BARBARA OLMI

INAF

OSSERVATORIO ASTRONOMICO DI PALERMO

– OSSERVATORIO ASTROFISICO DI ARCETRI

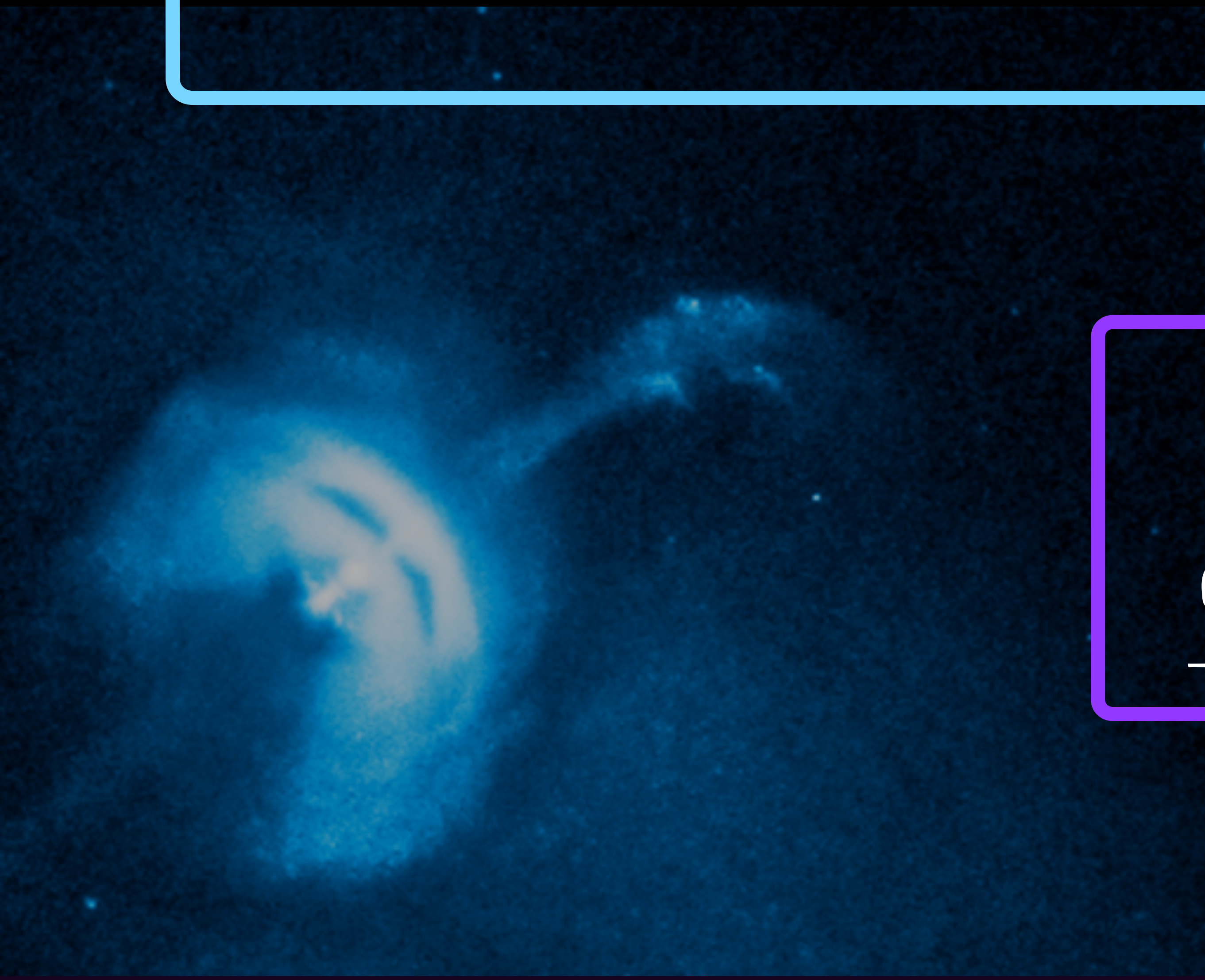

1-3 December 2020 - 1st Workshop on Gamma-ray Halos around Pulsars

THE THREE PHASES OF PWNe EVOLUTION

1 EARLY EVOLUTION – YOUNG PWN

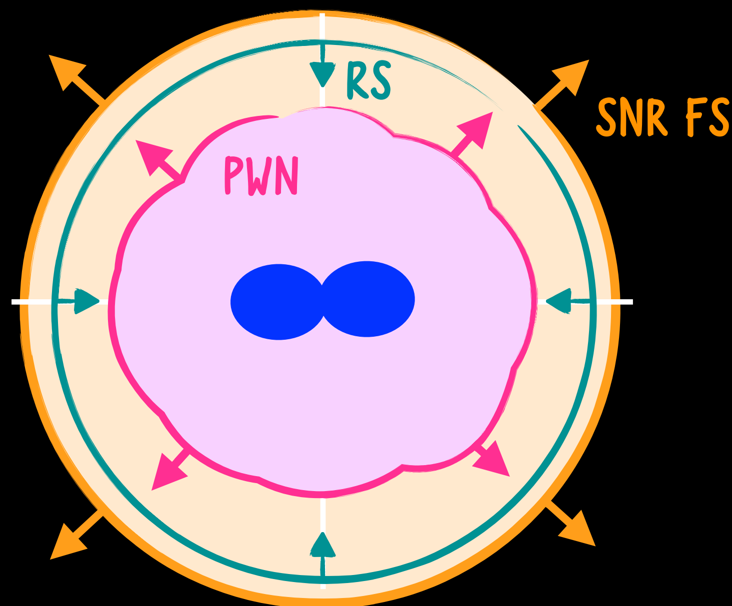

The PWN expands in the freely expanding ejecta (mild acceleration approaching linear expansion).

Phase ends when the Reverse Shock of SNR reaches the PWN.

[Studied with multiple approaches from one zone to multi-d simulations: Pacini & Salvati 1973, Reynolds & Chevalier 1984, van der Swaluw et al. 2001 , Bucciantini et al. 2003, Komissarov 2004, Del Zanna et al. 2006, Gaensler & Slane 2006, Martin et al. 2012, Olmi et. al 2014-15-16, Porth et al. 2014…]

2 REVERBERATION – MIDDLE AGED PWN

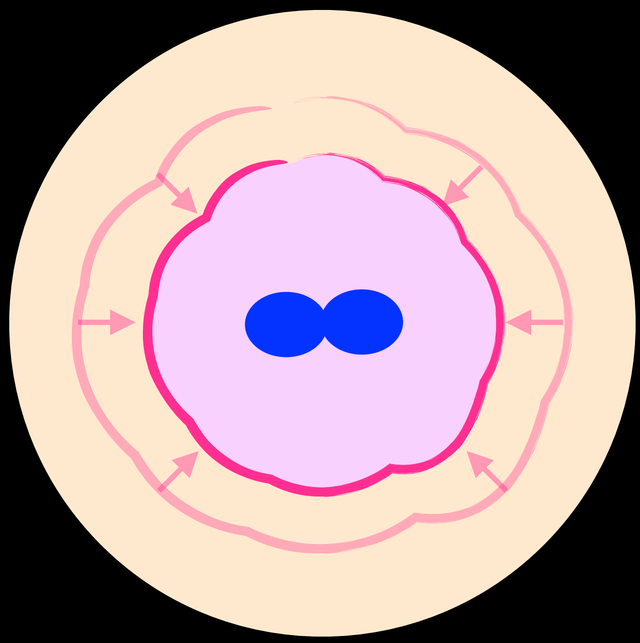

Complex interaction between PWN and SNR, eventually producing compression of the PWN.

[For a recent discussion see Bandiera et al. 2020]

3 POST-REVERBERATION: EVOLVED PWN

EVOLVED PWNe

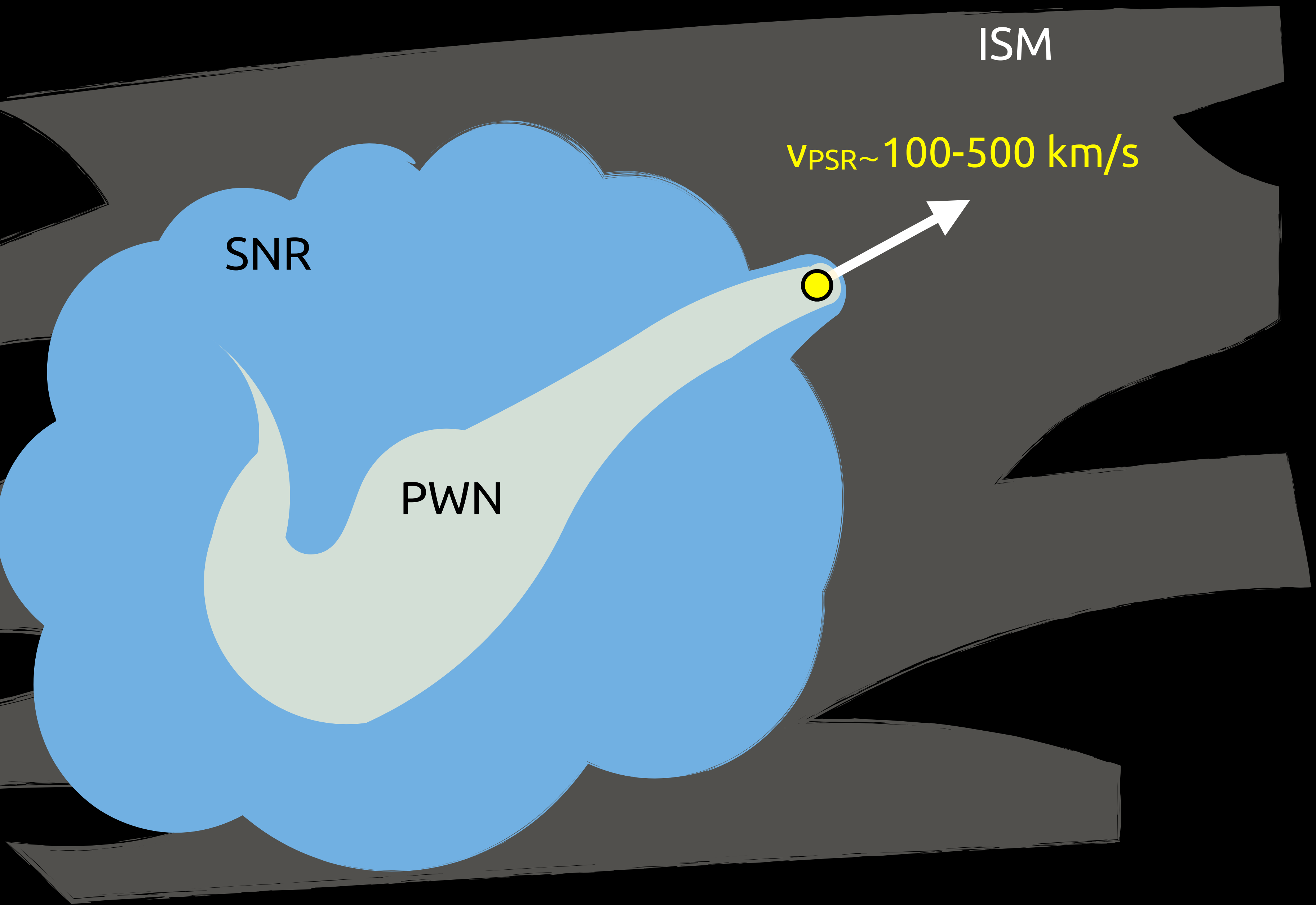

A large fraction of all the pulsars born with a high kick velocity (10%-50%) [Faucher-Giguere & Kaspi 2006]

↓

fated to escape the SNR on timescales << than typical pulsar ages (~10^6 yr)

BOW SHOCK PWNe

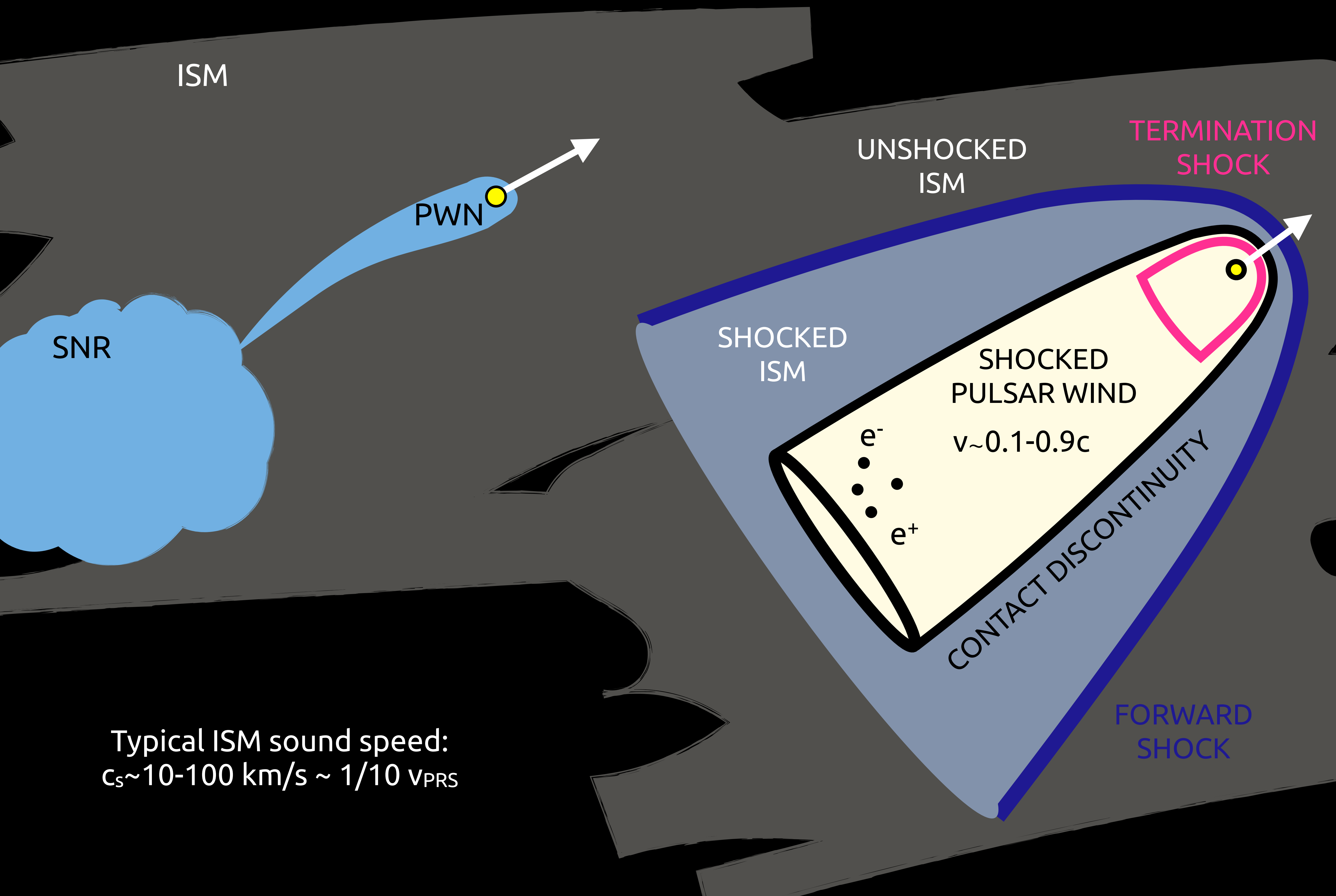

Typical ISM sound speed:
c_S~10-100 km/s ~ 1/10 v_{PRS}

THE COMETARY SHAPE of BSPWNe

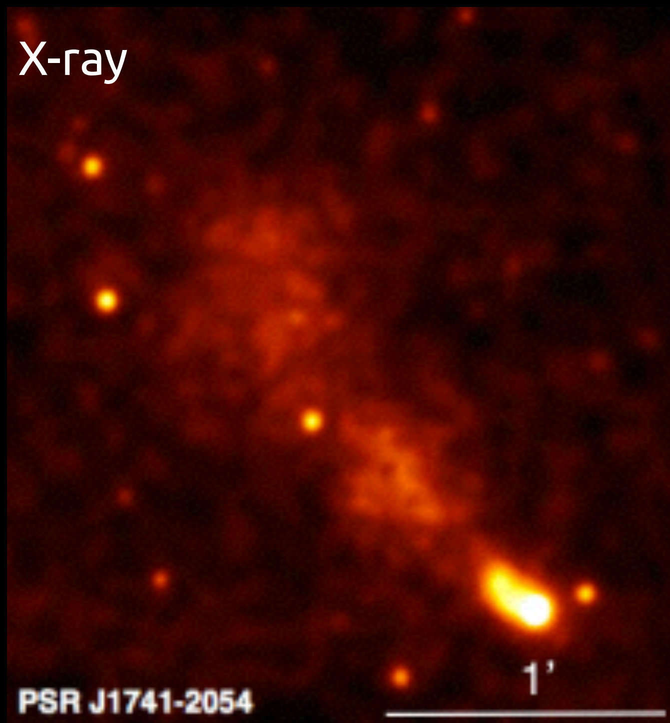

PSR J1741-2054
[Kargaltsev et al. 2016]

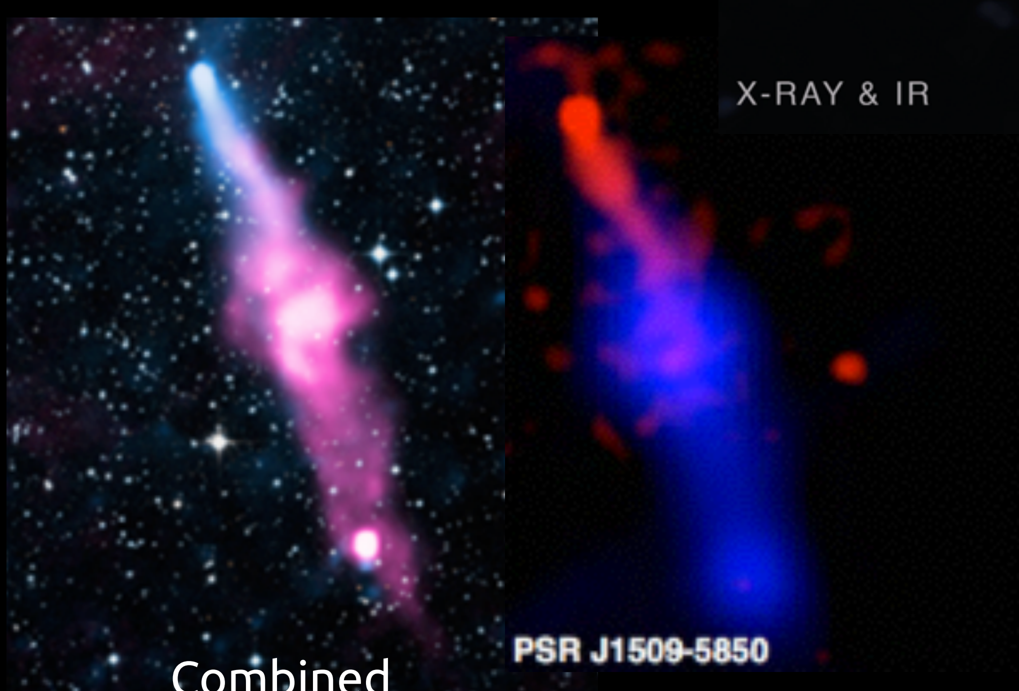

PSR J1509-5850
[Hui & Becker 2007, Klinger et al. 2016]

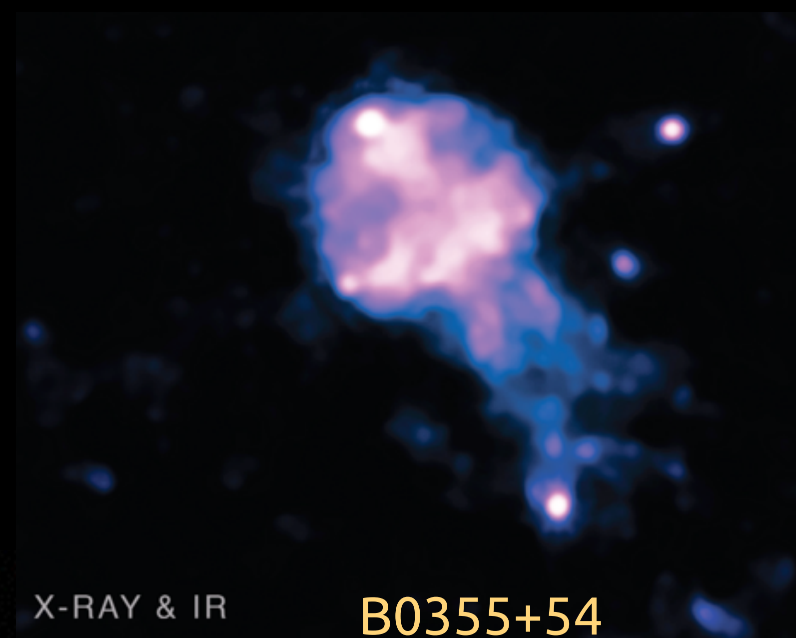

B0355+54
[Emre et al. 2005]

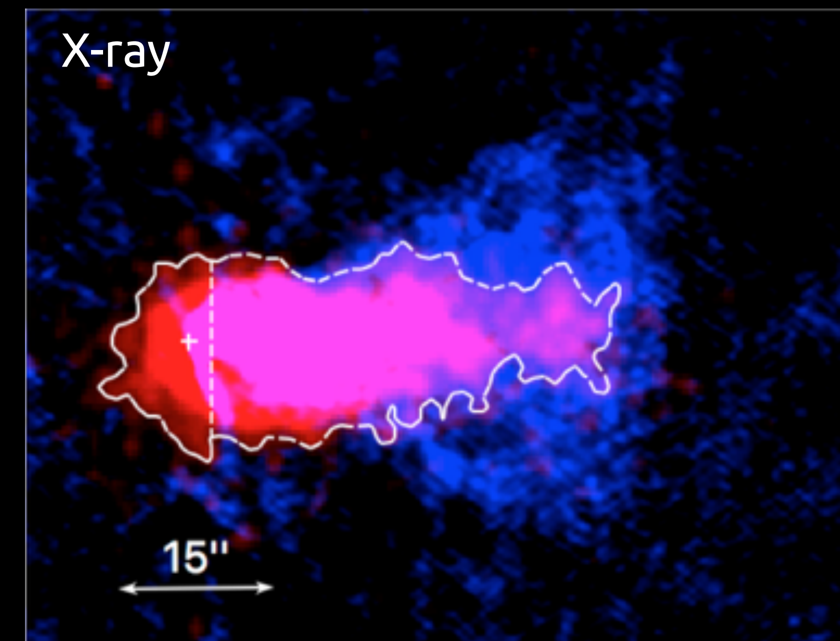

Mouse PWN
[Yusef-Zadeh & Bally 1987,
Yusef-Zadeh & Gaensler 2005,
Klinger et al. 2018]

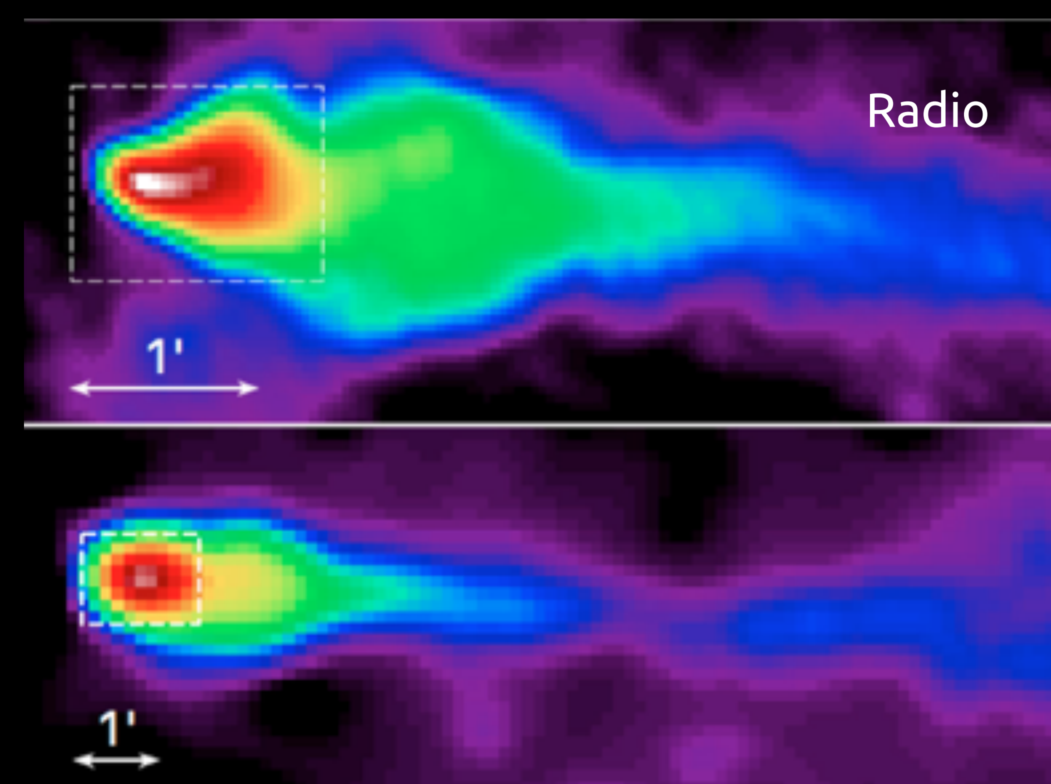

BSPWNe as SOURCEs of ENERGETIC PARTICLEs?

Extended TeV halos surrounding evolved pulsars

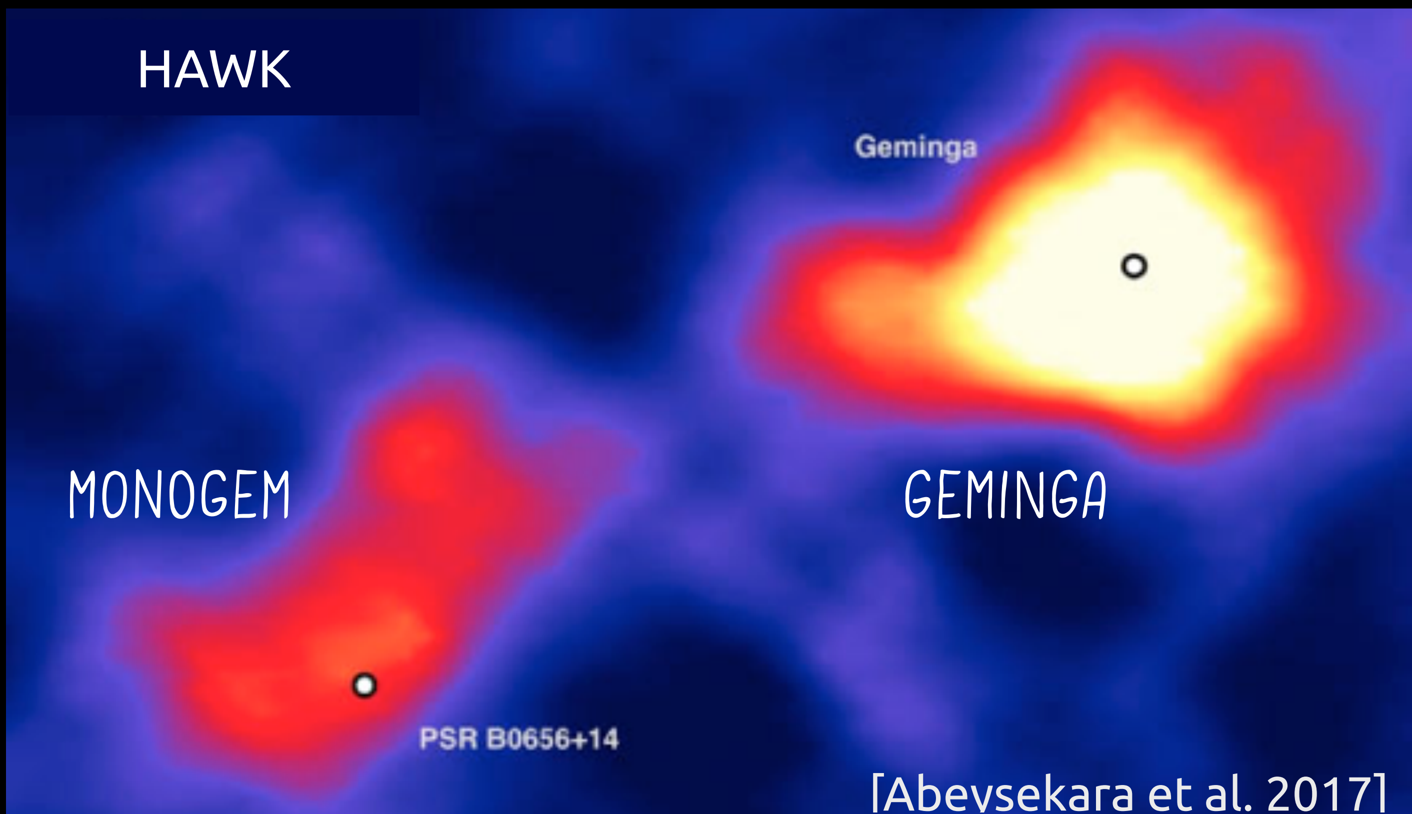

Asymmetric X-ray jets

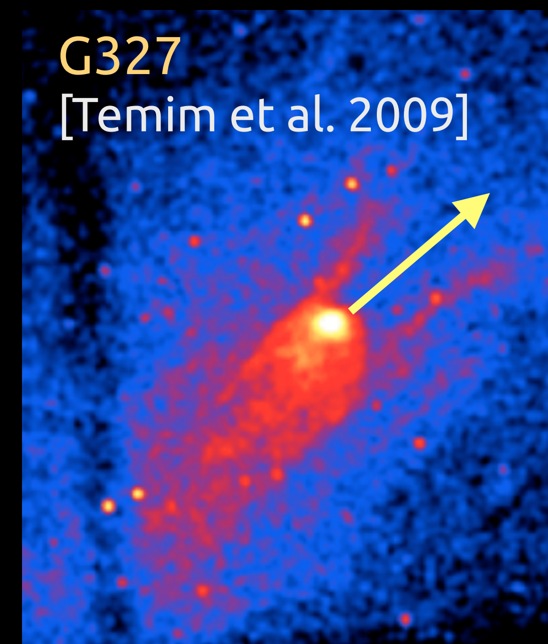

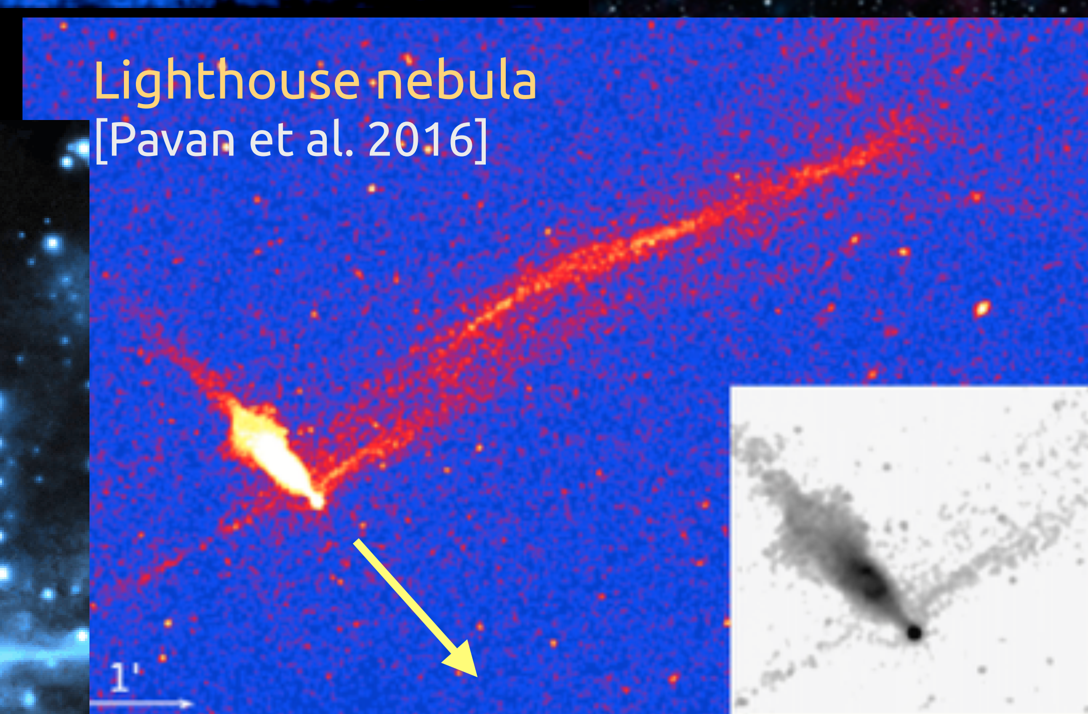

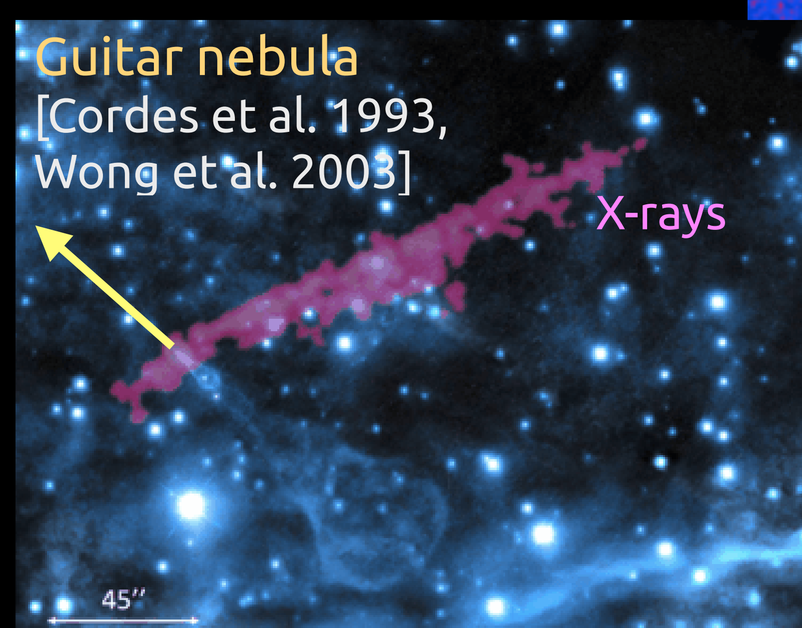

Other recent observations in:
J1809-1917 [Klinger et al. 2020]
J2030+4415 [de Vries & Romani 2020]
B1929+10 [Kim et al. 2020]

3D MHD SIMULATIONs of BSPWNe

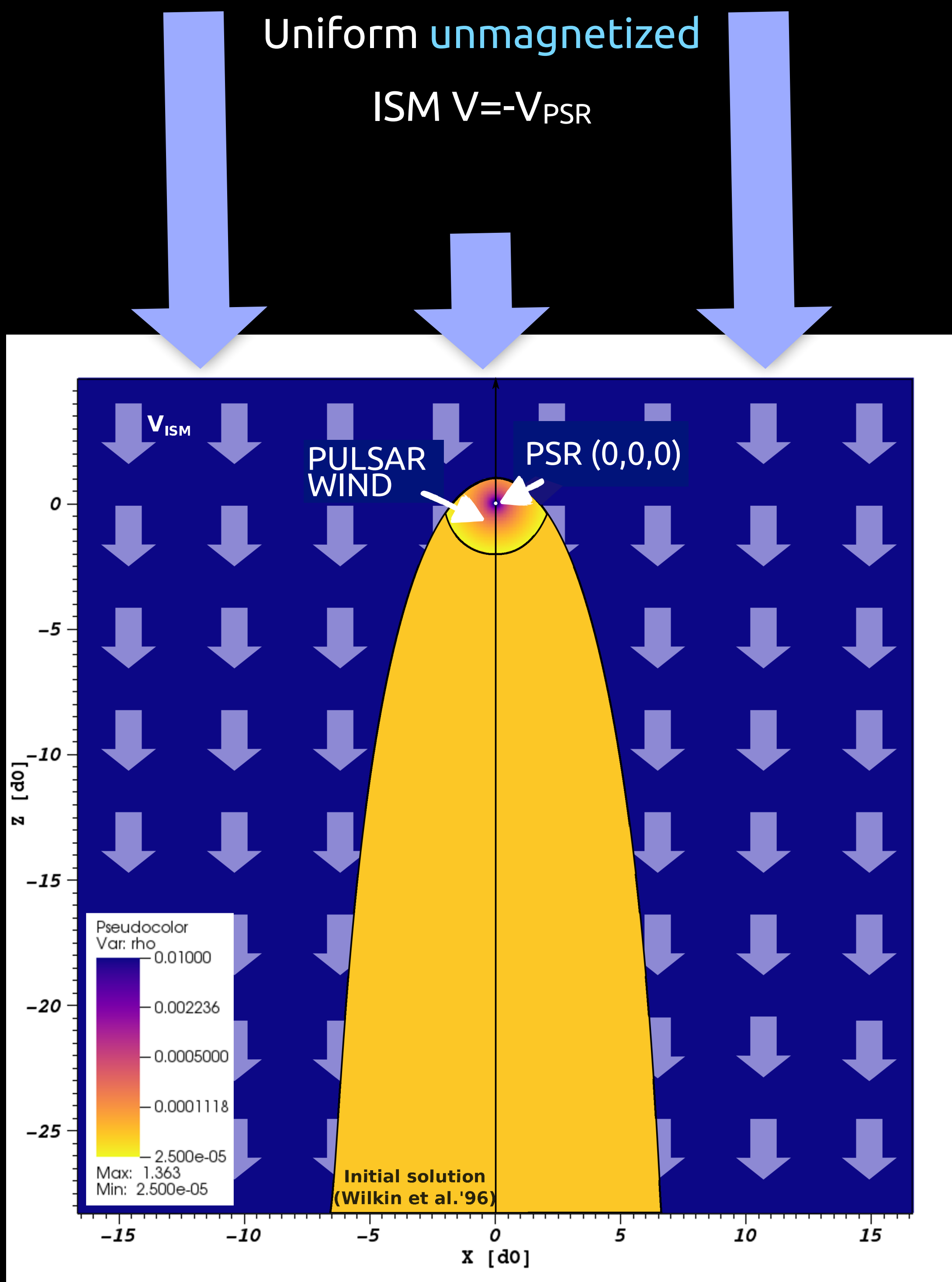

[Olmi & Bucciantini 2019a]

High resolution required to resolve the PW injection region and allow the TS to correctly detach from the inner boundary (use of Adaptive Mesh Refinement - AMR)

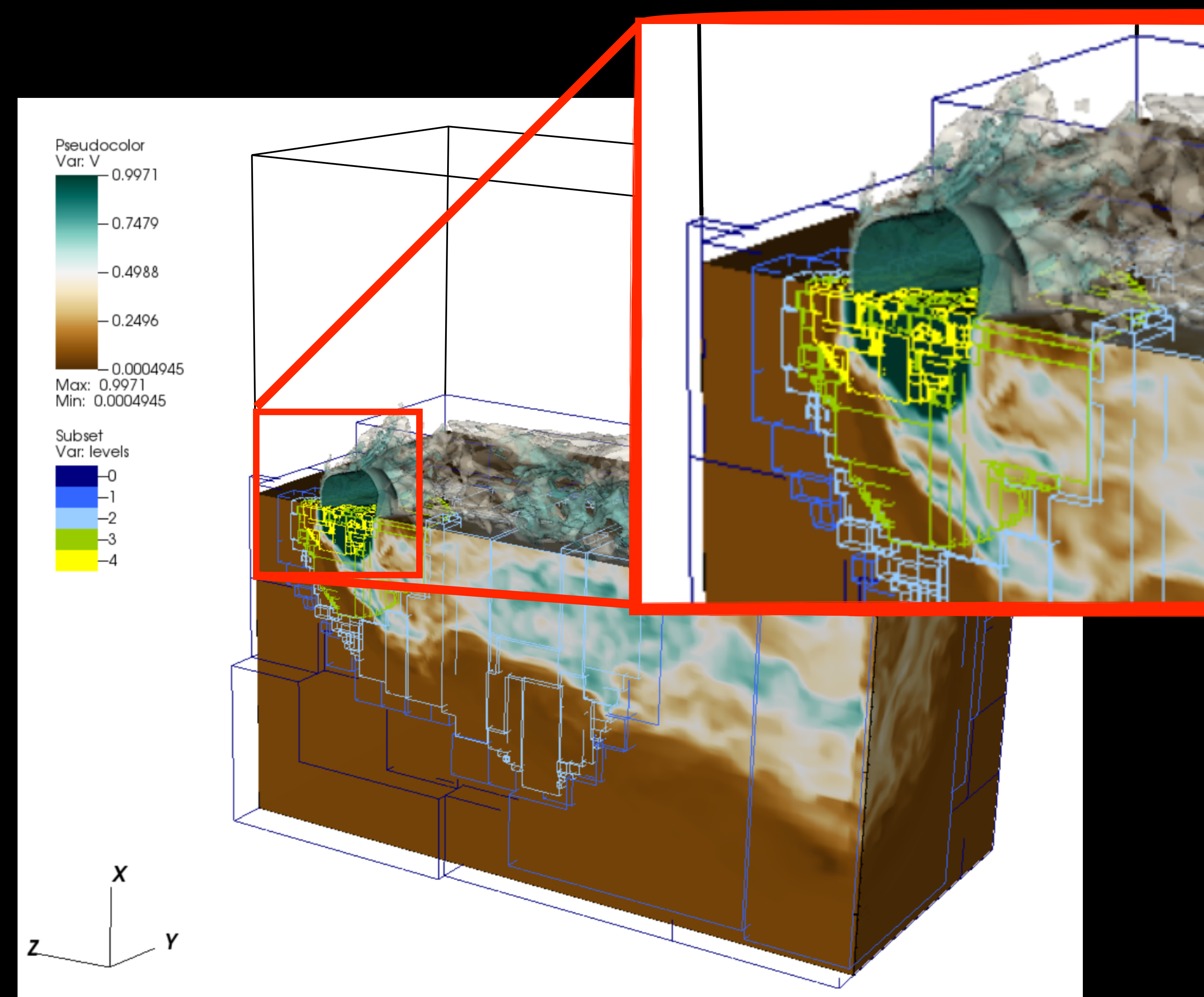

The numerical tool is the **PLUTO code** [Mignone et al. 2007]

Simulations supported by
MoU INAF-CINECA
class A projects

MODELING THE PULSAR WIND AND GEOMETRY

DISTRIBUTION OF ENERGY

Energy flux as function of the colatitute from the spin axis:

$$F(\psi) \propto 1 + \alpha \sin^2 \psi$$

$\alpha = 0 \Longrightarrow$ isotropic
$\alpha \neq 0 \Longrightarrow$ anisotropic

WIND MAGNETIZATION

σ= magnetic flux/kinetic flux=0.0, 0.01, 0.1, 1

GEOMETRY

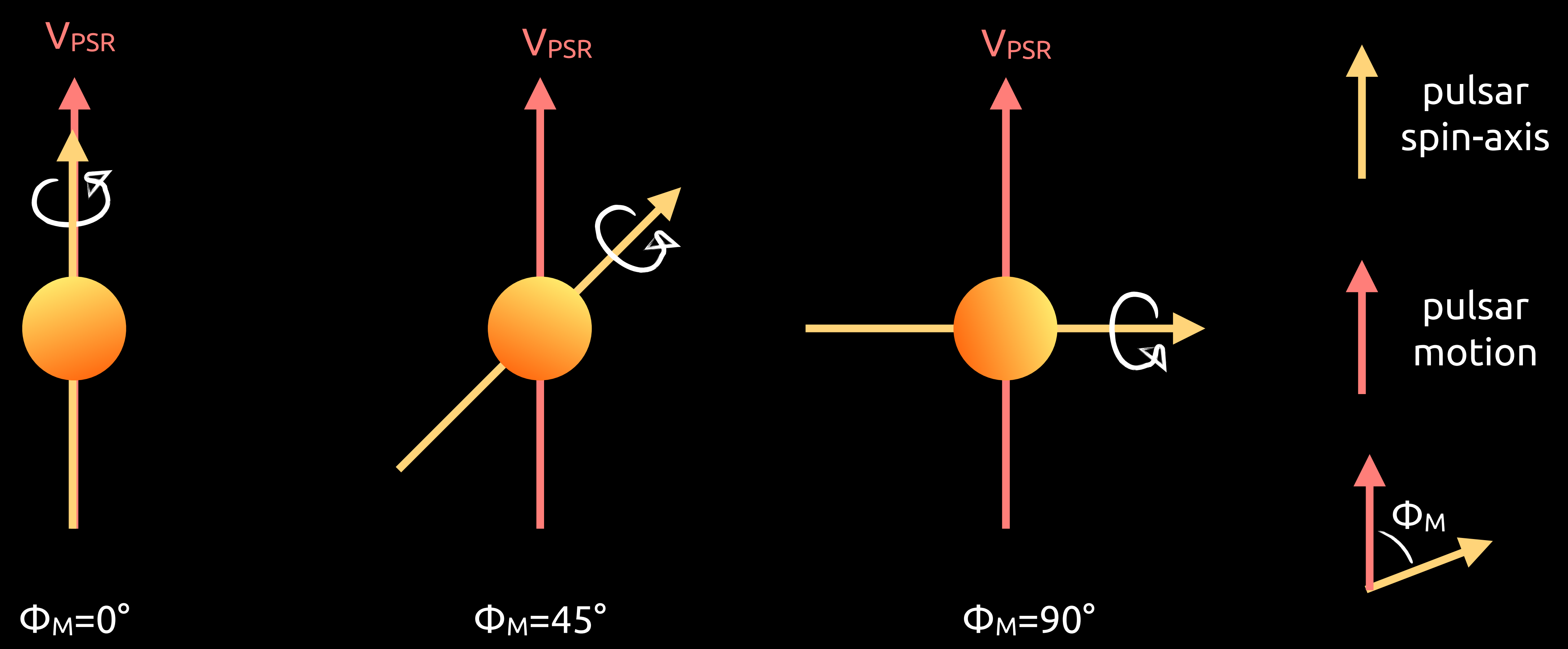

COMPARING DIFFERENT MODELS

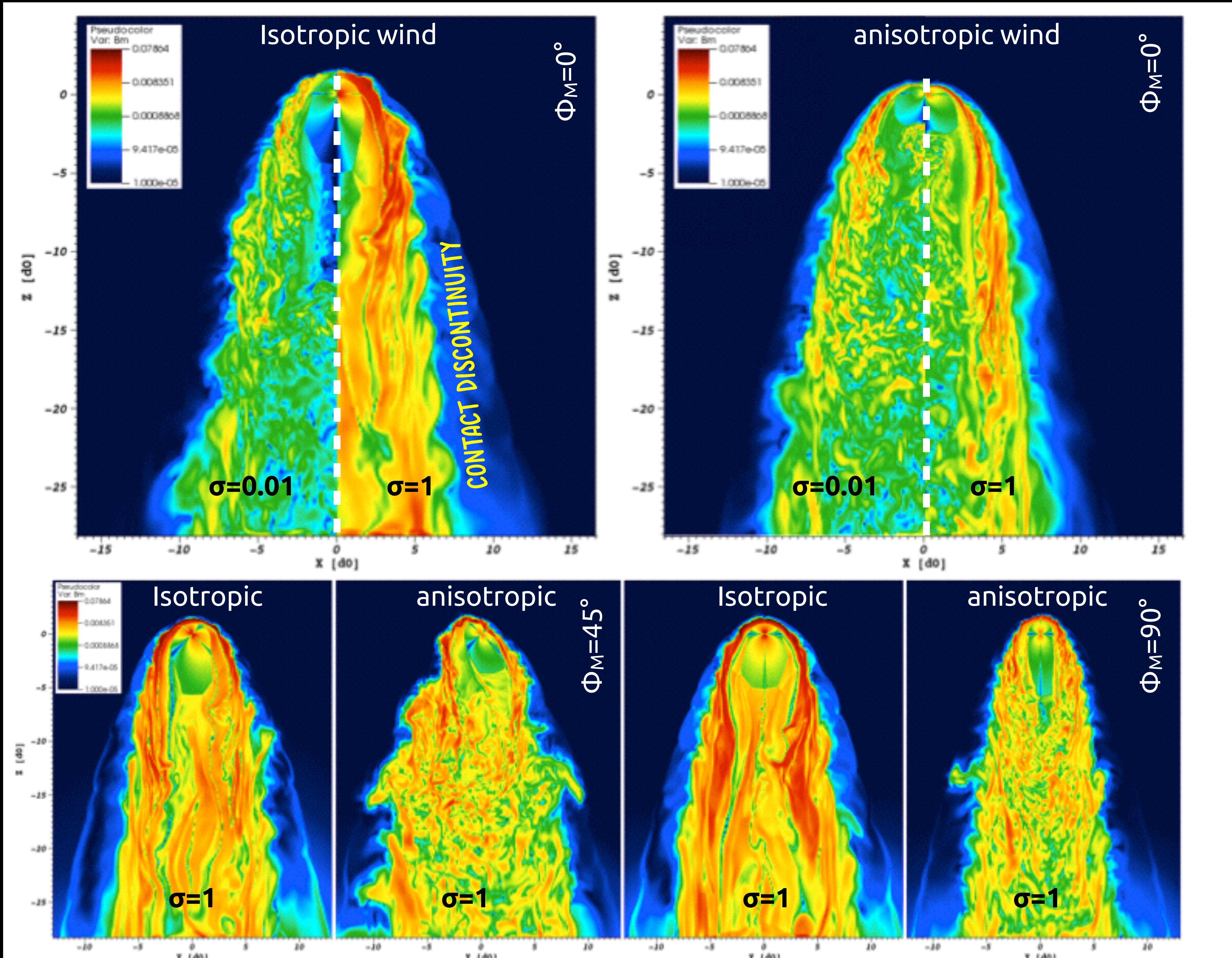

[Olmi & Bucciantini 2019a]

DEVELOPMENT OF TURBULENCE IN TAILS

ISOTROPIC WIND

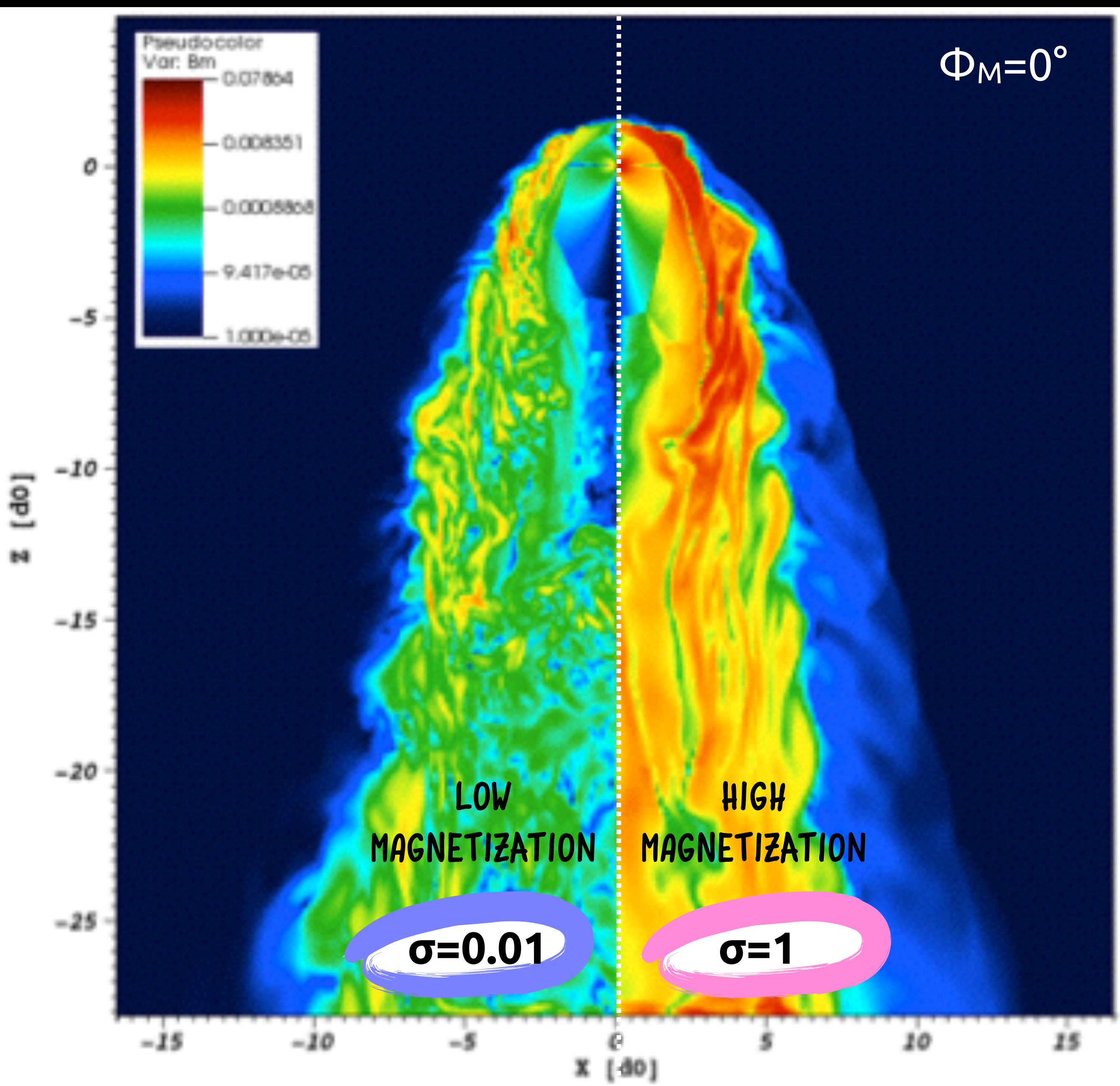

HIGH LEVEL OF TURBULENCE
CHAOTIC FLOW

LOW LEVEL OF TURBULENCE
LAMINAR FLOW

ANISOTROPIC WIND

DEVELOPMENT OF TURBULENCE IN TAILS

ISOTROPIC WIND

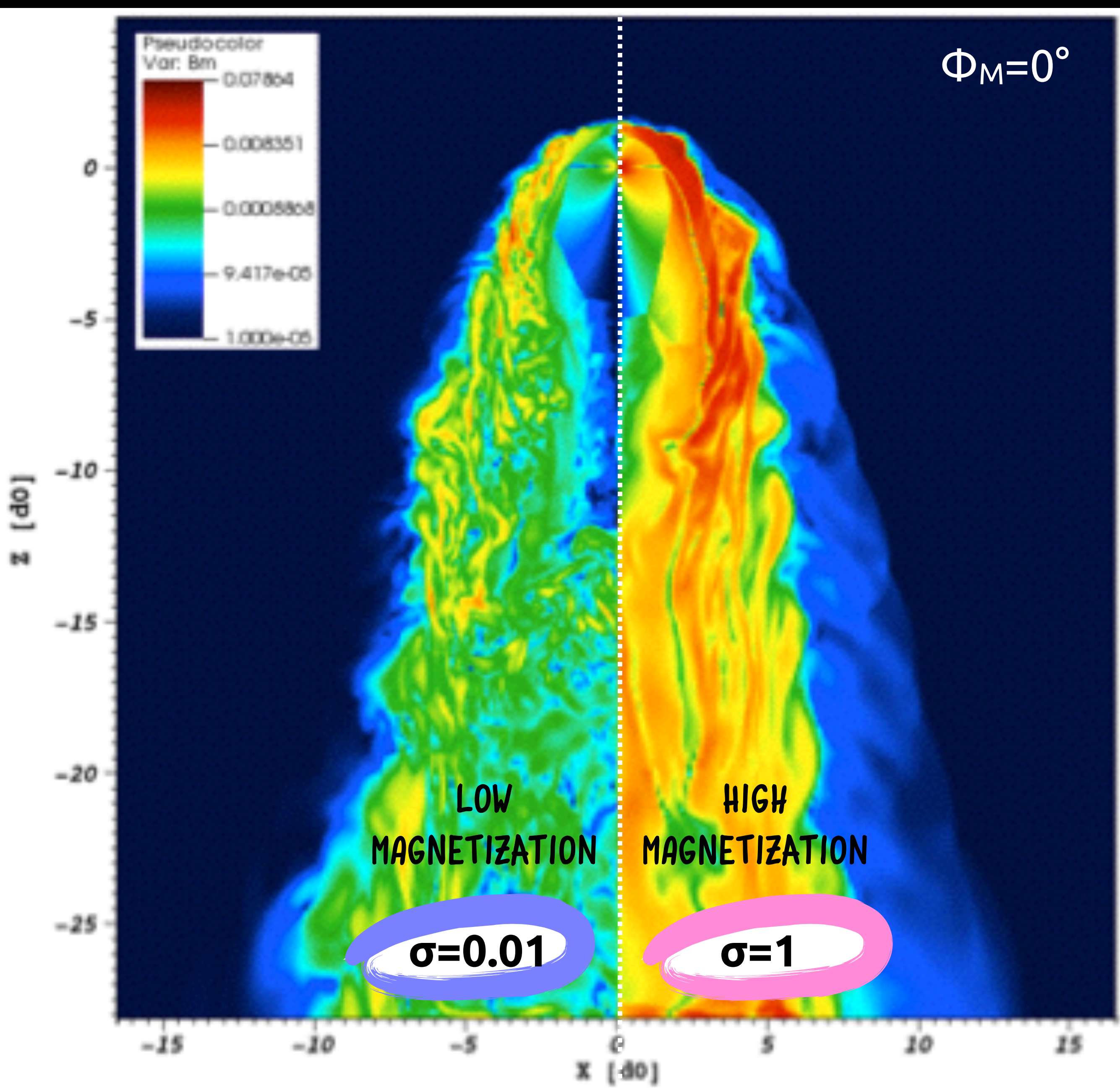

HIGH LEVEL OF TURBULENCE
CHAOTIC FLOW

LOW LEVEL OF TURBULENCE
LAMINAR FLOW

ANISOTROPIC WIND

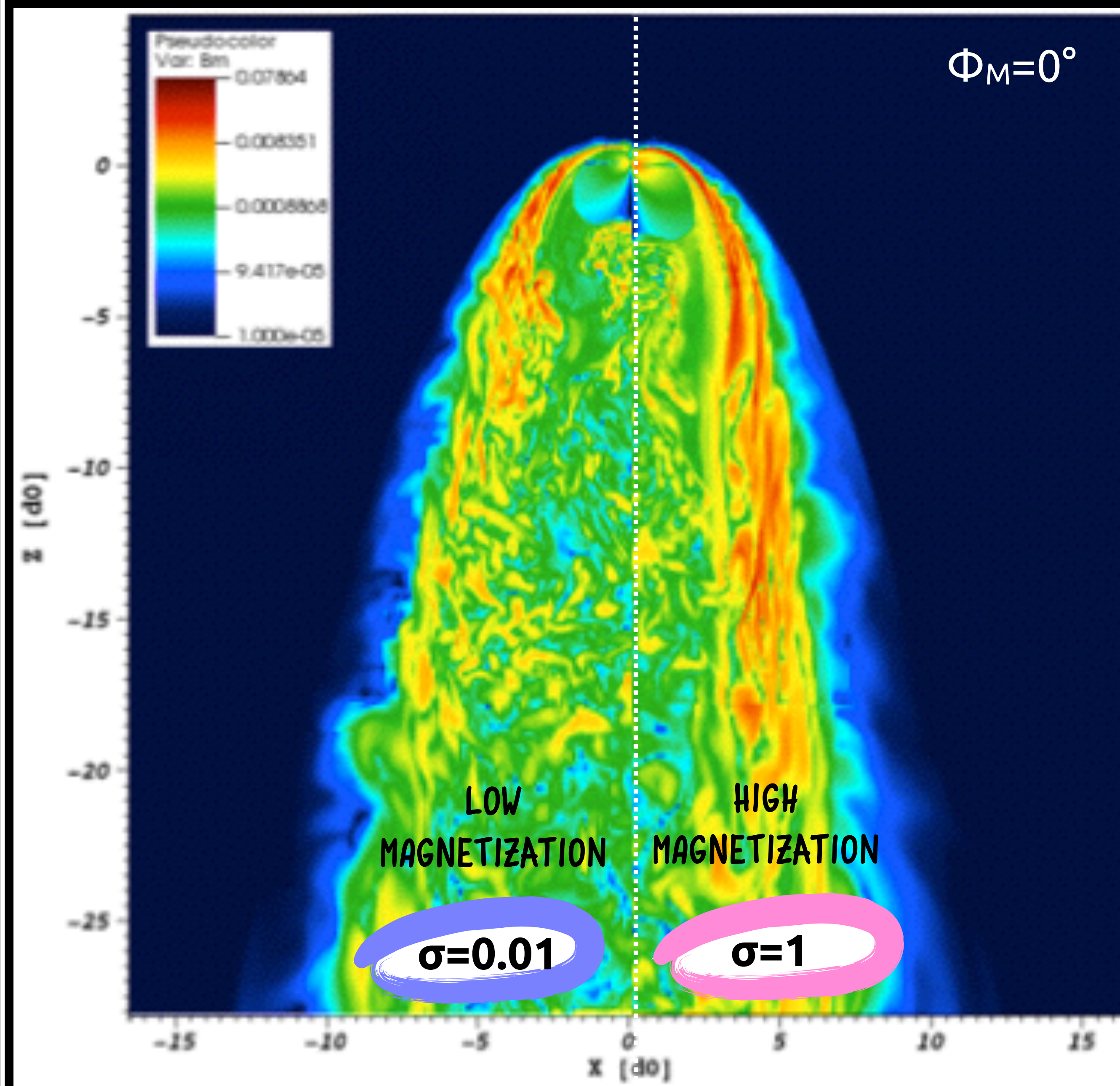

LESS MARKED DIFFERENCE IN ANISOTROPIC WINDS

DEVELOPMENT OF TURBULENCE IN TAILS

ISOTROPIC WIND

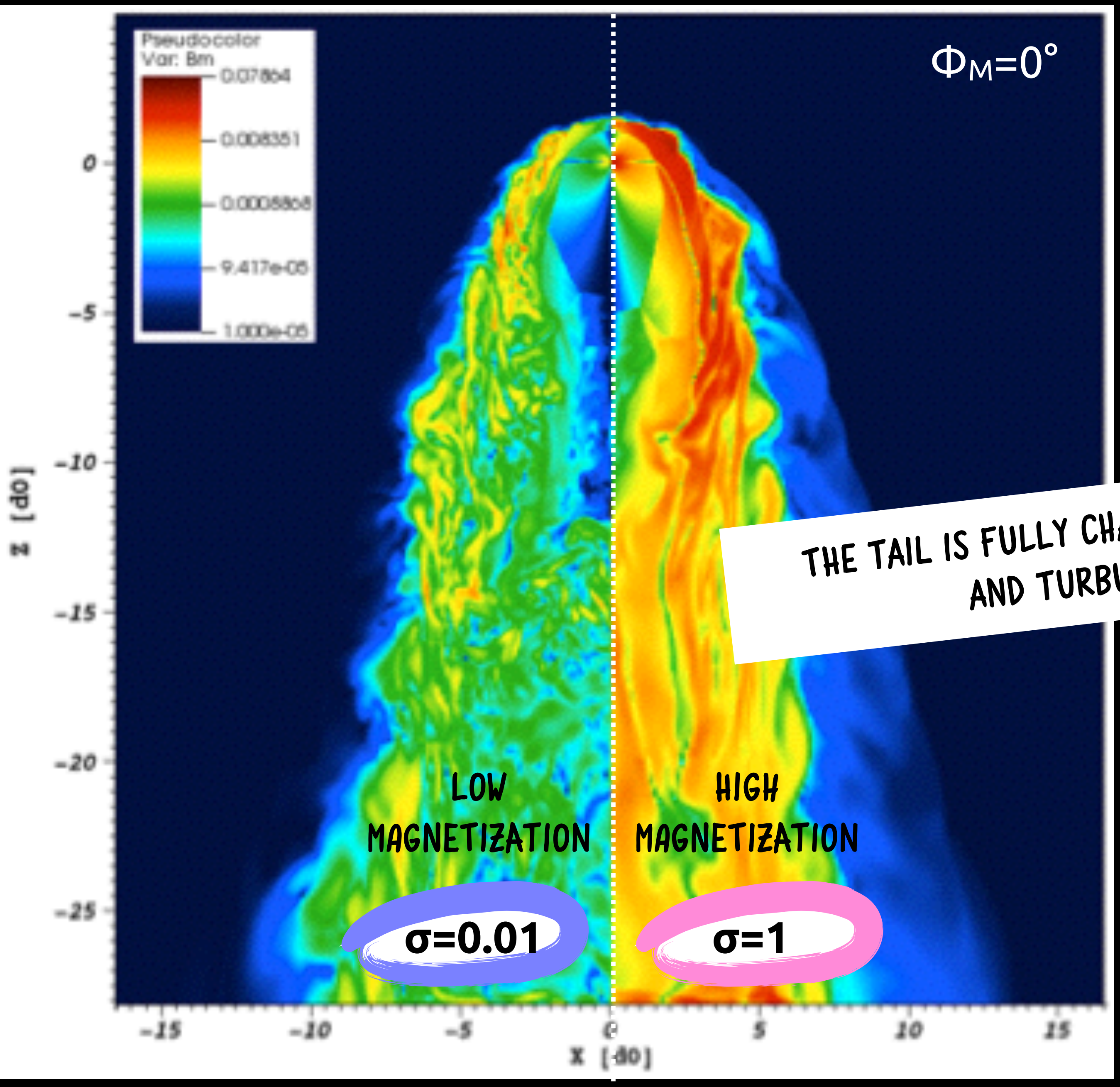

ANISOTROPIC WIND

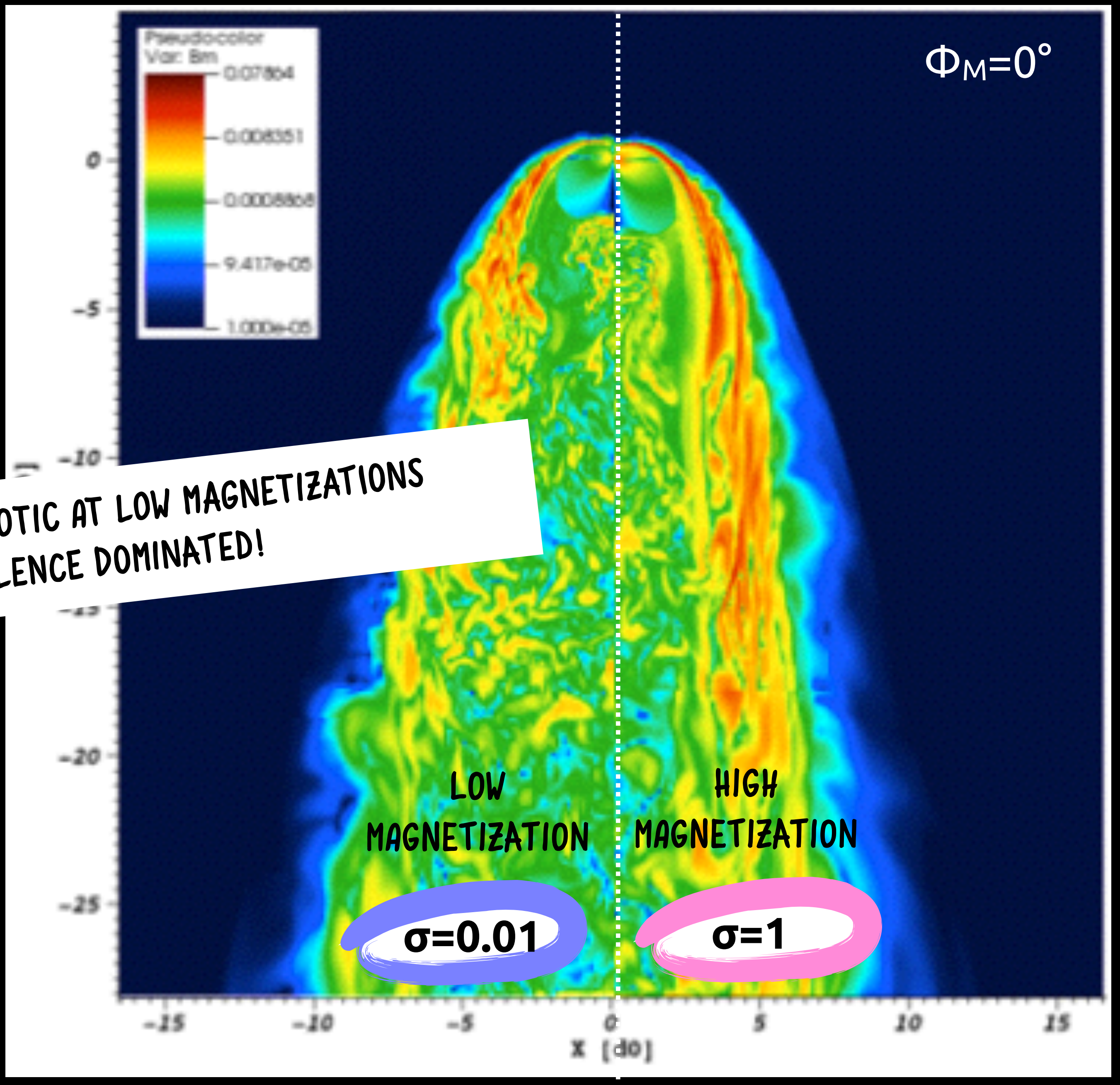

THE TAIL IS FULLY CHAOTIC AT LOW MAGNETIZATIONS AND TURBULENCE DOMINATED!

TAIL DYNAMICS FOR HIGH MAGNETIZATION (σ=1)

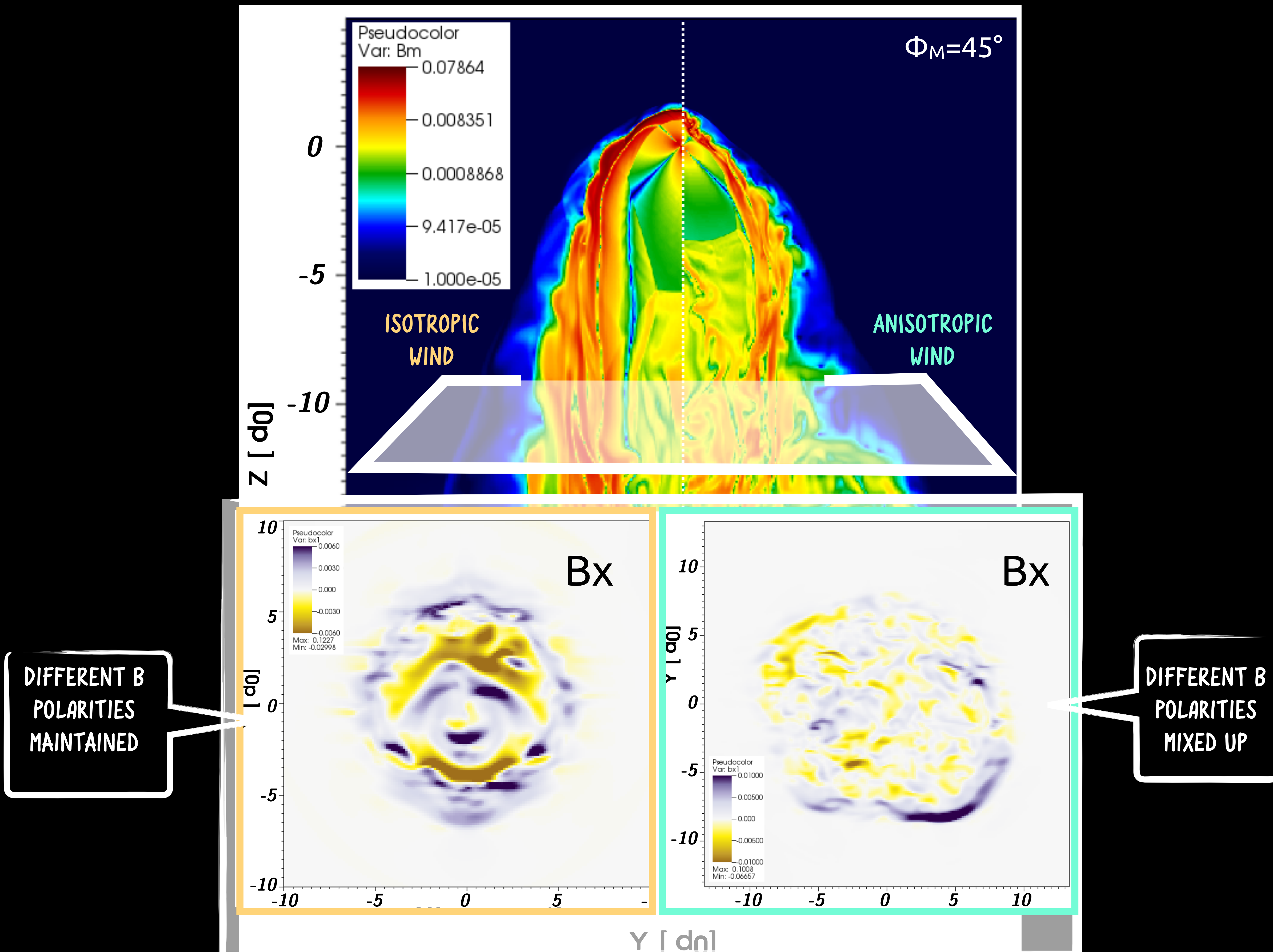

SURVIVAL OF CURRENT SHEETS IN THE TAIL

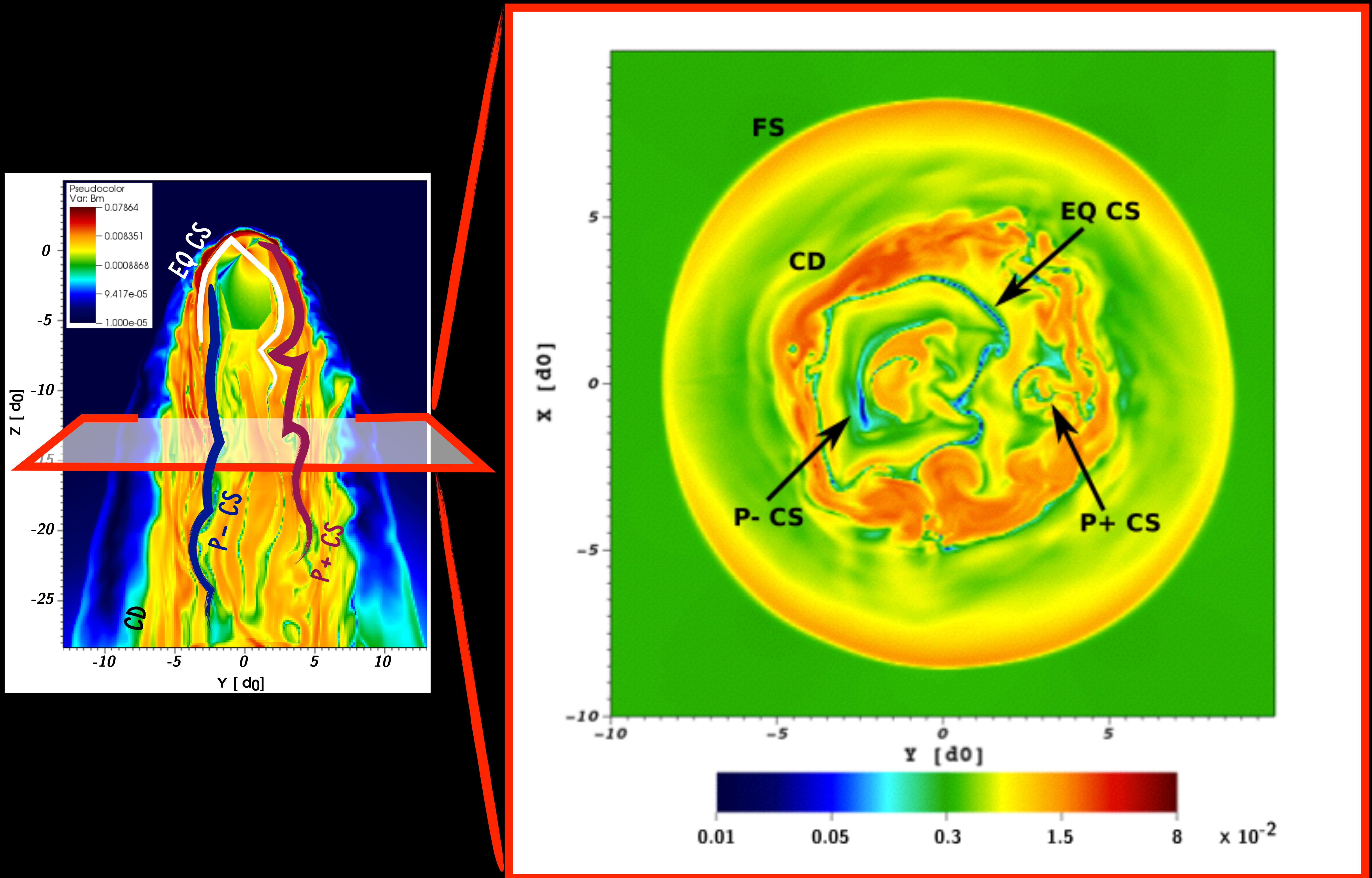

[Olmi & Bucciantini 2019c]

SWITCHING ON THE FIELD

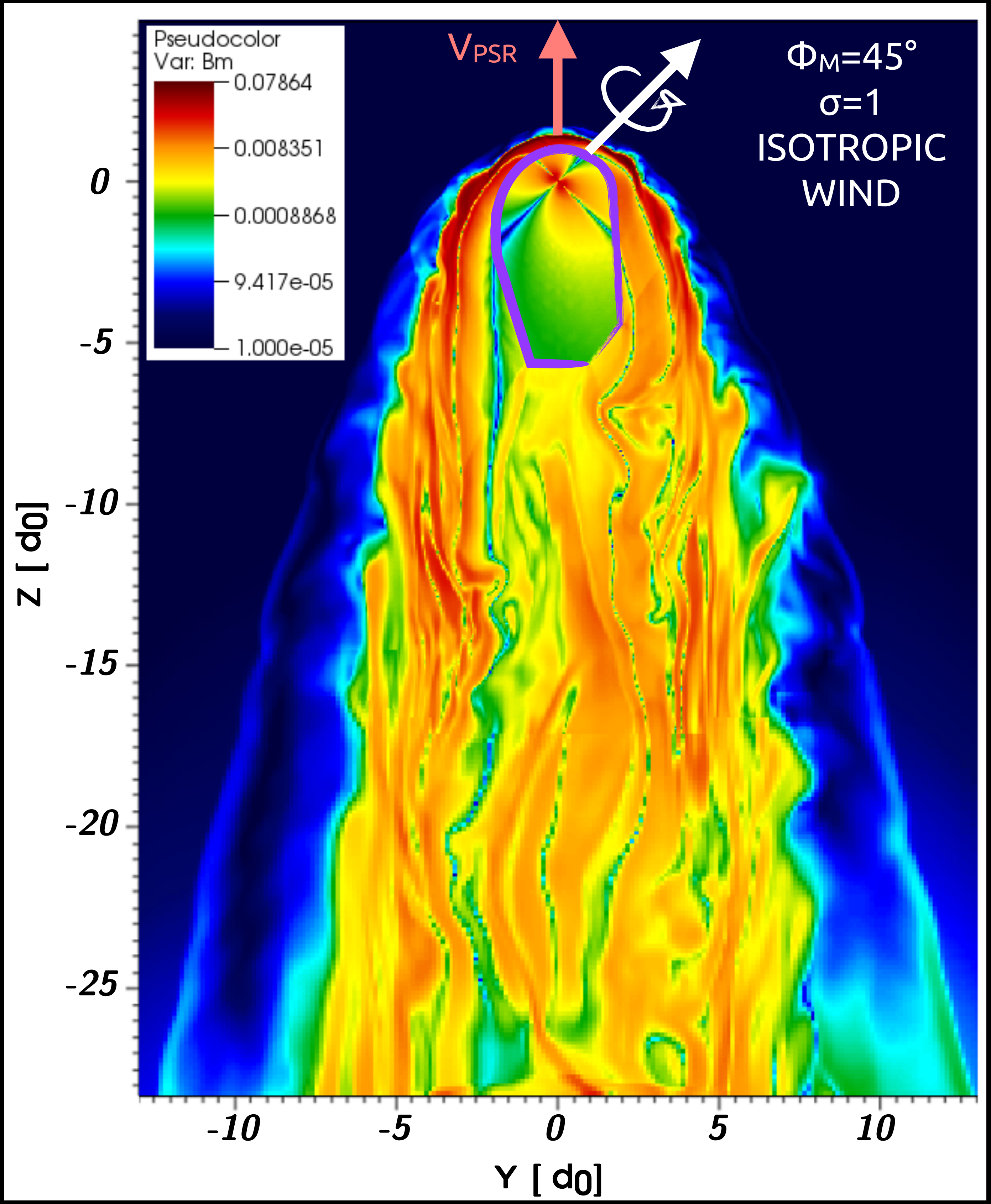

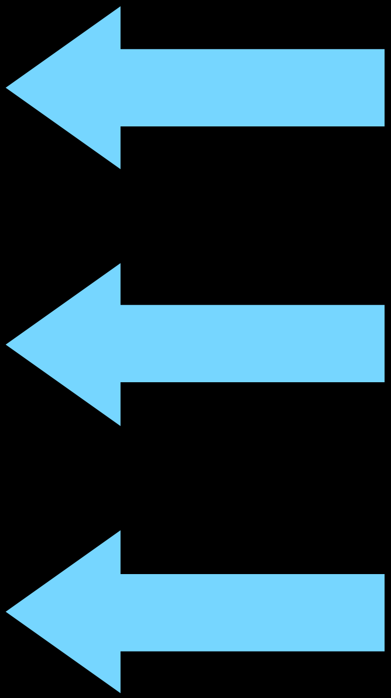

B ISM

$|B|=0.01\rho_{ISM}v_{PSR}\sim$ 3-5 μG

INJECTING PARTICLES

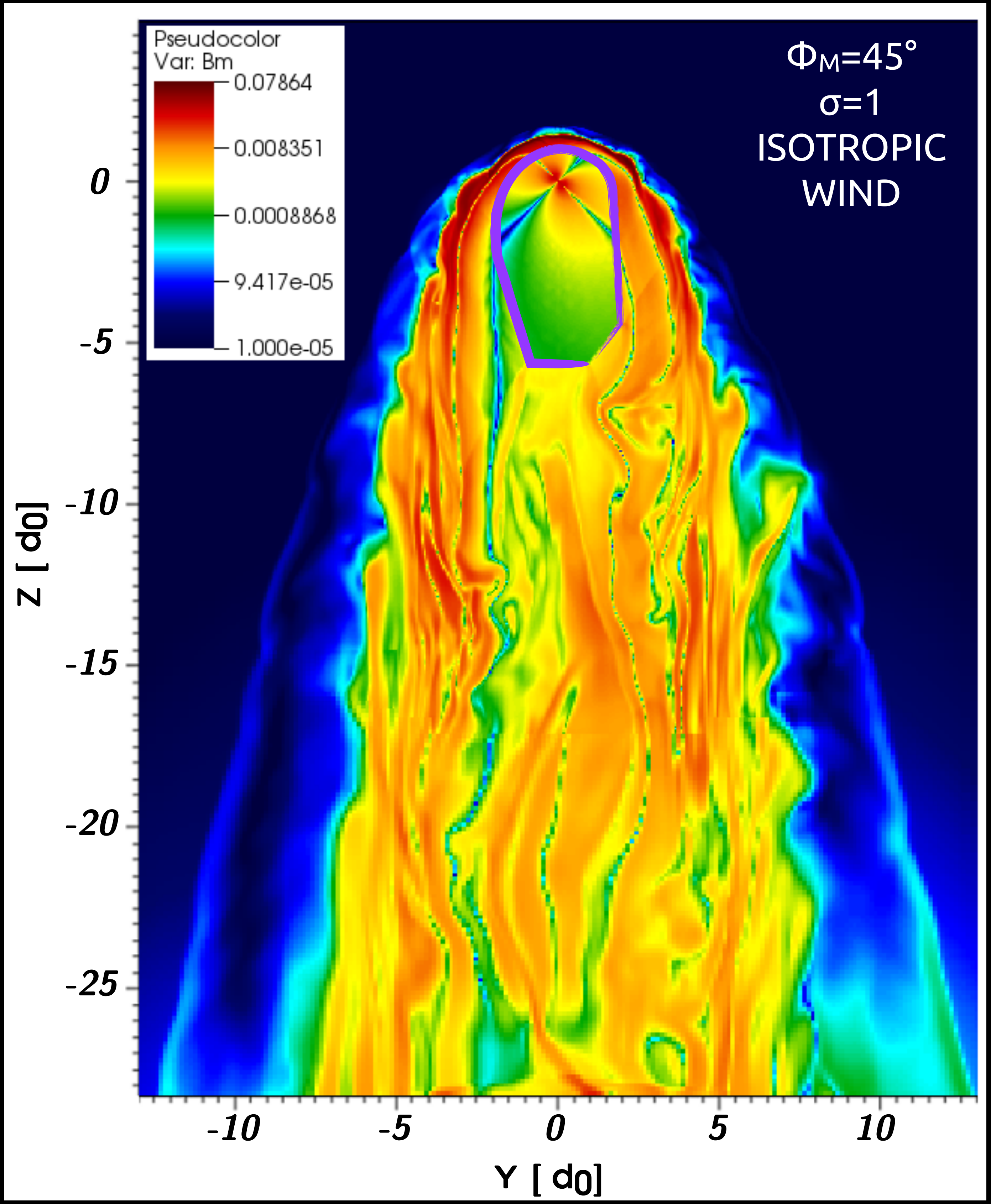

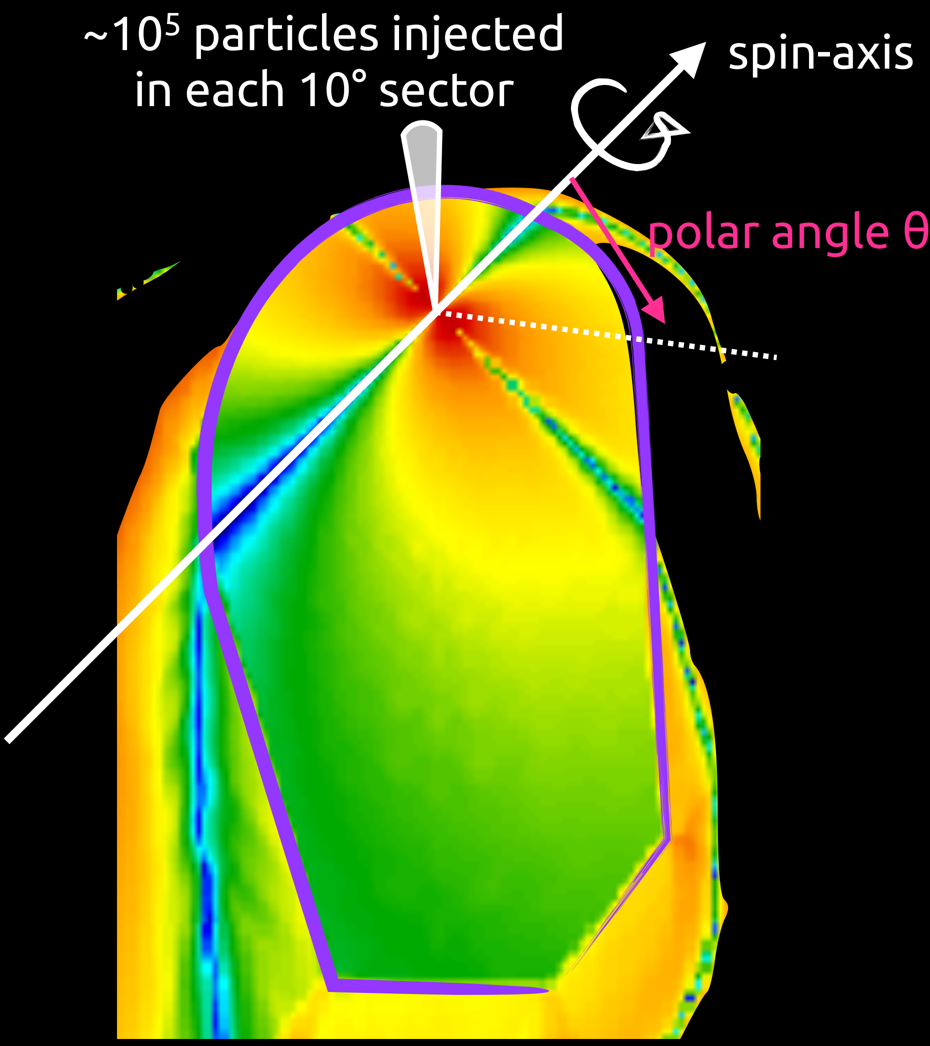

Electrons and positrons of different energies (from TeV to ~50 TeV):

$\gamma = E/(m_e c^2) = [0.5, 1.0, 3.0, 10] \times 10^7$

PARTICLES MOSTLY ESCAPE FROM THE FRONT-POLAR FLOW

Particles remain confined in current sheets.
The polar flow points directly to the magnetopause and then particles can more efficiently jump on ISM field lines.

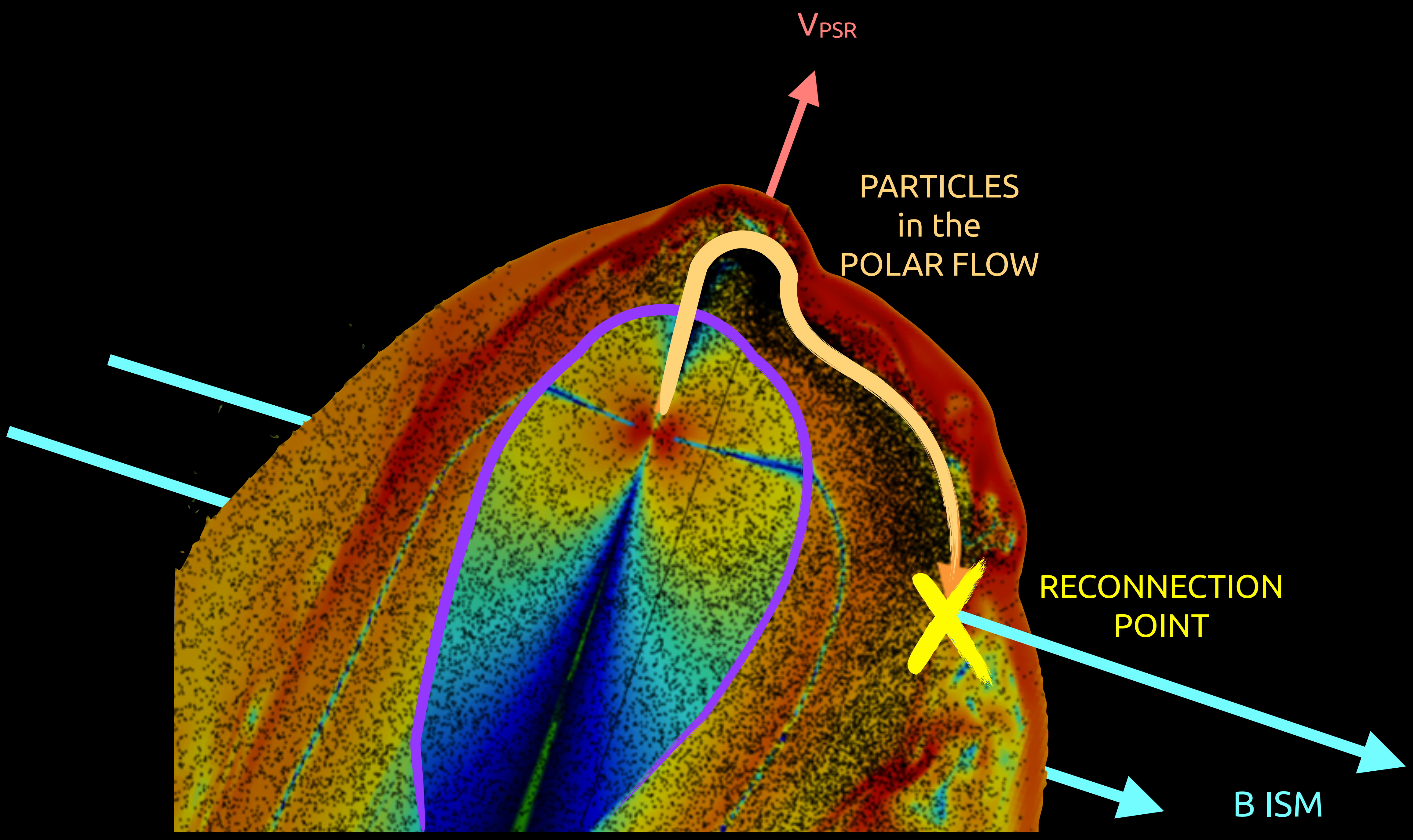

[Barkov et al. 2019, Bucciantini 2018, Olmi & Bucciantini 2019c]

EFFICIENCY OF ESCAPE

Escape efficiency is energy dependent:

low energy particles are tightly attached to field lines and marginally escape only through sporadic reconnection points

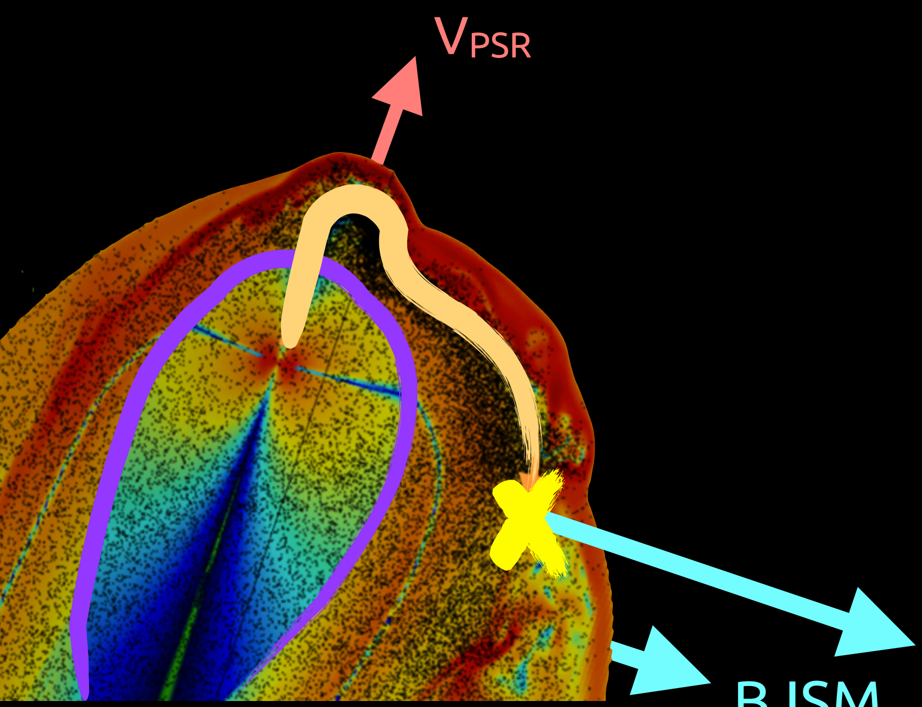

ESCAPE EFFICIENCY

$$R_L \text{ vs } d_0 = \sqrt{\dot{E}/(4\pi c \rho_{ISM} v_{PSR}^2)} \sim 10^{16}\,\text{cm}$$

ALMOST 0

$R_L/d_0 \lesssim 0.1$

$\gamma \lesssim 10^6$

HIGH

$R_L/d_0 > 0.1$

$\gamma > 10^6$

ENERGY of ESCAPING PARTICLES

1 TeV — 10 TeV — 10ns of TeV

← confinement

escape →

[Barkov et al. 2019, Bucciantini 2018, Olmi & Bucciantini 2019c]

THE ESCAPE PROCESS IS ENERGY DEPENDENT

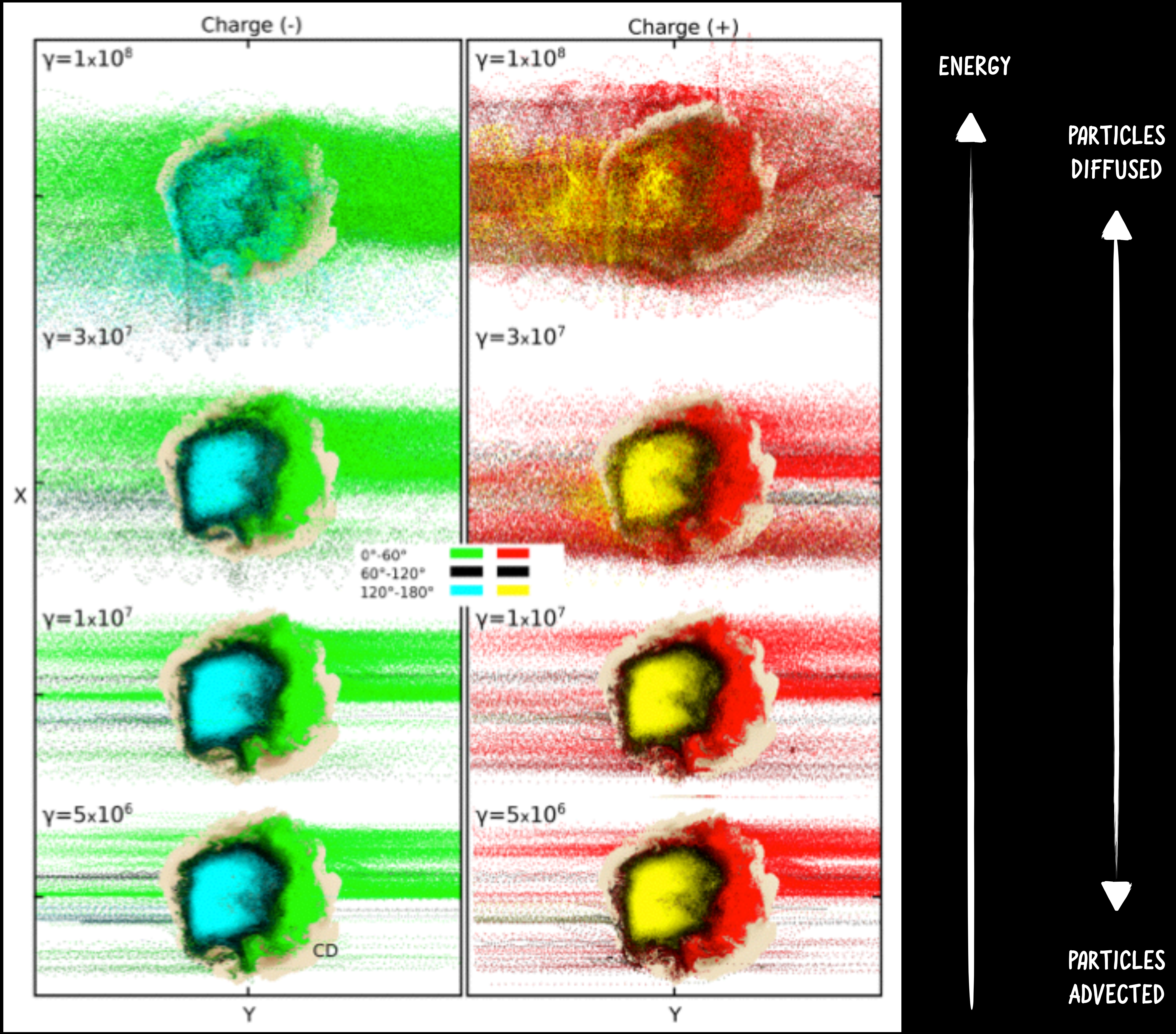

THE ESCAPE PROCESS IS ENERGY DEPENDENT

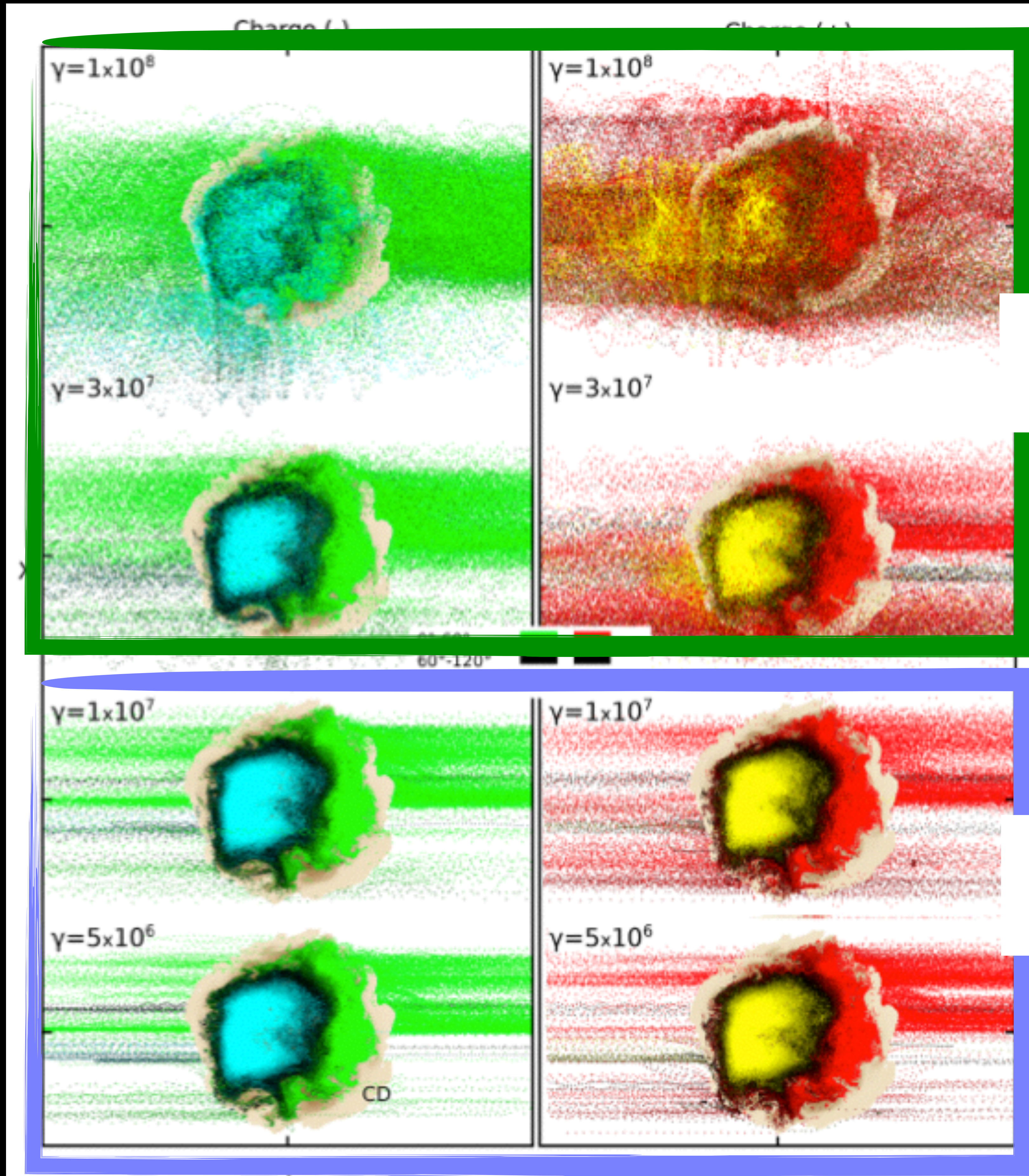

ENERGY

PARTICLES DIFFUSED

UP TO 100% OF PARTICLES INJECTED IN THE FRONT-POLAR FLOW ESCAPE AND PARTIALLY FROM OTHER SECTORS

ONLY FEW % OF PARTICLES INJECTED IN THE FRONT-POLAR FLOW ESCAPE

PARTICLES ADVECTED

PARTICLES LEAKAGE IS CHARGE DEPENDENT AND ASYMMETRIC

Particles escape as seen from tail:

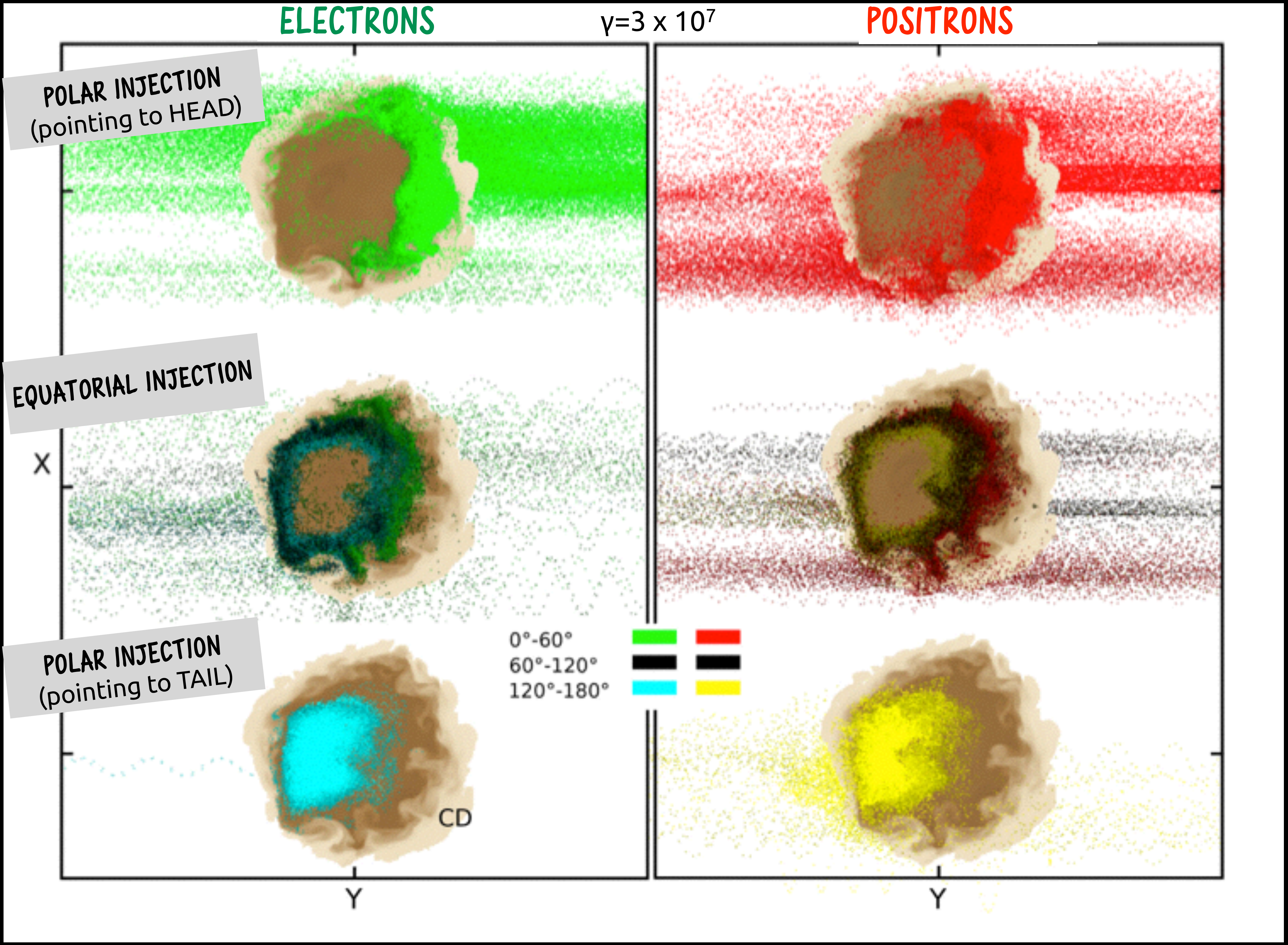

ESCAPE IN LARGE FRACTIONS

PARTLY CONFINED

HIGHLY CONFINED

[Olmi & Bucciantini 2019c]

FORMATION OF JETS OR HALOS

[Olmi & Bucciantini 2019c]

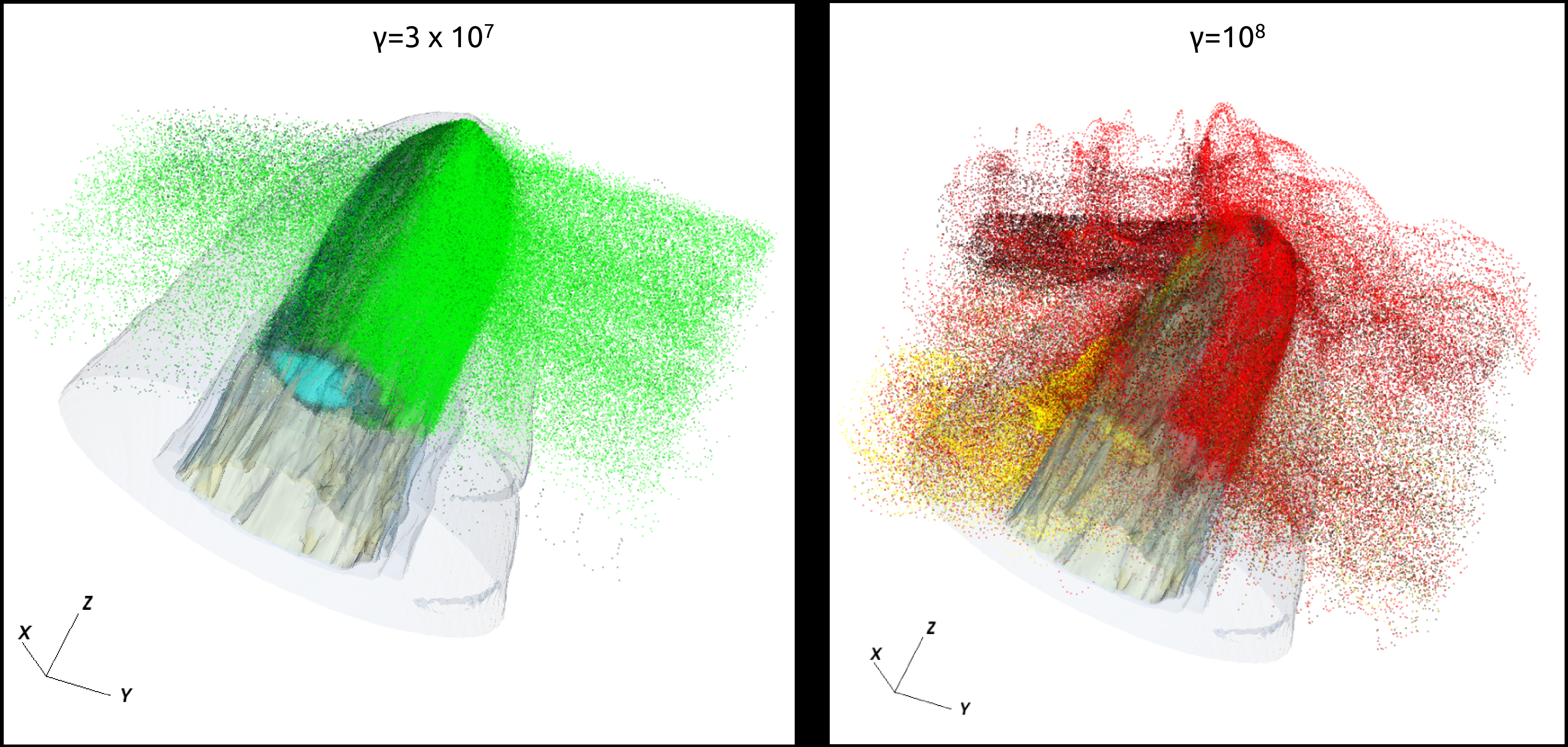

Particles can efficiently escape from BSPWNe + escape is energy and charge dependent:

- sporadic escape of LOW ENERGY particles through reconnection points between PWN and ISM B field. Escape strongly asymmetric (depeding on the system geometry). The charge asymmetry is small (~10%).

- HIGH ENERGY particles enter a diffusive regime when r_L ~ thickness of the current sheet. Now the escape flow is less asymmetric but strongly charge separated.